creative commons
COMMONS DEED

저작자표시-비영리-변경금지 2.0 대한민국

이용자는 아래의 조건을 따르는 경우에 한하여 자유롭게

- 이 저작물을 복제, 배포, 전송, 전시, 공연 및 방송할 수 있습니다.

다음과 같은 조건을 따라야 합니다:

저작자표시. 귀하는 원저작자를 표시하여야 합니다.

비영리. 귀하는 이 저작물을 영리 목적으로 이용할 수 없습니다.

변경금지. 귀하는 이 저작물을 개작, 변형 또는 가공할 수 없습니다.

- 귀하는, 이 저작물의 재이용이나 배포의 경우, 이 저작물에 적용된 이용허락조건을 명확하게 나타내어야 합니다.
- 저작권자로부터 별도의 허가를 받으면 이러한 조건들은 적용되지 않습니다.

저작권법에 따른 이용자의 권리는 위의 내용에 의하여 영향을 받지 않습니다.

이것은 이용허락규약(Legal Code)을 이해하기 쉽게 요약한 것입니다.

Disclaimer

dCollection

의학박사 학위논문

Evaluation of the Therapeutic Effect of Cytosine Deaminase-Expressing Mesenchymal Stem Cells and 5-Fluorocytosine on Glioma using Molecular Imaging

분자영상을 이용한 Cytosine Deaminase 발현 줄기세포와 5-Fluorocytosine 의 악성 뇌교종 치료효과 평가

2016 년 2 월

서울대학교 대학원

의과학과 의과학전공

정 태 문

A thesis of the Degree of Doctor of Philosophy

분자영상을 이용한 Cytosine Deaminase 발현 줄기세포와 5-Fluorocytosine 의 악성 뇌교종 치료효과 평가

Evaluation of the Therapeutic Effect of Cytosine Deaminase-Expressing Mesenchymal Stem Cells and 5-Fluorocytosine on Glioma using Molecular Imaging

February 2016

The Department of Medical Science

Seoul National University

Graduate School

Tae Moon Chung

ABSTRACT

Introduction: Despite advances in chemotherapy and radiation after tumor resection, the high propensity of glioma cells to invade the surrounding normal brain tissue reduces the survival rate of patients The therapeutic use of mesenchymal stem cells (MSCs) has recently been extensively investigated in cancer therapy because of these cells tumor targeting properties. In this study, the efficacy of combination therapy using MSCs expressing cytosine deaminase (CD) and prodrug 5-FC in a mouse glioma model was evaluated using various molecular imaging modalities.

Methods: Human glioma cell lines (U373, U87MG) and primary glioblastoma cells from a patient (GBM28) were stably transfected with fluorescent and luciferase reporter genes for tumor cell imaging. Glioma cells were treated with standard therapy (ionizing radiation, Temozolomide (TMZ)) or 5-FU in a dose dependent manner. Microarray and real-time PCR were performed to determine the expression levels of radio-resistant and 5-FU metabolism related genes. Therapeutic MSC/CDs were established by the transfection of CD genes into human bone-marrow derived MSCs. Next, i*n vitro* and *in vivo* 19F-magnetic resonance spectroscopy (19F-MRS) was performed to estimate the conversion of 5-FC to 5-FU by the MSC/CDs. To validate the *in vitro* anticancer effect of MSC/CDs with 5-FC, luciferase-expressing glioma cells were co-cultured with MSC/CDs. For in vivo monitoring of the therapeutic effect of MSC/CDs with 5-FC, U87MG/Luc cells were inoculated into the mouse cranium. Consequently, therapeutic MSC/CD were transplanted into the mouse cranium. Tumor growth was measured using bioluminescence imaging (BLI), magnetic resonance imaging (MRI) and positron emission tomography (PET).

Results: Glioma cells and MSCs were successfully monitored using fluorescence and BLI. U87MG cells were killed following exposure to ionizing radiation (3 Gy), with a survival rate of

82.8% ± 9.59%, while U373 and GBM28 ells had a survival rate of 57.9% ± 6.88% and 48.0% ± 6.0%. In contrast, 36.3% ± 8.9% of U87MG cells survived after 5-FU treatment (4 uM), whereas 68.6% ± 15% of U373 cells survived. Unlike in ionizing radiation studies, U87MG cells were found to be two times more sensitive to 5-FU than U373 cells. Microarray analysis demonstrated that U87MG cells highly express DNA repair-related genes compared to U373 cells. The expression of rate-limiting enzymes of 5-FU metabolism in U87MG cells is low. *In vitro* and *in vivo* studies of 19F-MRS revealed the effective conversion of 5-FC to 5-FU by MSC/CDs. Based on a co-culture experiment with MSC/CDs and glioma cells, MSC/CDs showed an anticancer effect on neighboring cancer cells in proportion to increasing the 5-FC dosage and the MSC/CD ratio. The *in vitro* anticancer effects of MSC/CD therapy with 5-FC on U87MG cells were two times more effective than on U373 cells. In a glioma orthotopic model, a BLI/MRI/PET molecular imaging system revealed 70% inhibition of tumor growth by MSC/CD with 5-FC therapy. Furthermore, no tumorigenesis or pathological abnormalities were observed at the MSC/CD transplantation site.

Conclusions: Taken together, the efficacy of a new stem cell mediated enzyme/prodrug therapy was determined using various imaging modalities. In particular, BLI was able to accurately verify the therapeutic effect of MSCs in vitro and in vivo. In addition, the different response of therapeutic efficacy on glioma cells was revealed using microarray analysis. Therefore, the suggested MSC/CD and prodrug 5-FC therapy could be an effective anticancer therapy option for radio-resistant and 5-FU-sensitive glioma treatment.

Keywords: Glioblastoma, Mesenchymal stem cell, Cytosine Deamiase, Molecular imaging, 5-FU, 5-FC

Student number: 2011-30634

CONTENTS

LIST OF TABLES AND FIGURES

LIST OF ABBREVIATIONS

GBM, Glioblastoma multiforme

TMZ, Temozolomide

5-FU, 5-Fluorouracil

5-FC, 5-Fluorocytosine

CD, Cytosine deaminase

MSC, Mesenchymal stem cell

DPD, *Dihydropyrimidine dehydrogenase*

OPRT, *Orotate phosphoribosyl transferase*

TP, *Thymidine phosphorylase*

BLI, Bioluminescence imaging

MRI, Magnetic resonance imaging

PET, Positron emission tomography

11C-MET, 11C-methyl-$_L$-methionine

DMEM, Dulbecco's modified Eagle's medium

19F-MRS, 19F-Magnetic Resonance Spectroscopy

GFP, Green fluorescent protein

RFP, Red fluorescent protein

RT-PCR, Reverse transcriptase-polymerase chain reaction

FACS, Fluorescent activated cell sorting

INTRODUCTION

1. Standard Therapy for Glioblastoma

Glioblastoma is the most common malignant brain tumor and one of the most aggressive cancers (1, 2). It has been demonstrated that the median survival rate of glioma patients is generally less than one year from the time of diagnosis (3). A human clinical trial lead by the European Organization for Research and Treatment of Cancer (EORTC) recommends concomitant radiation therapy together with TMZ over radiation alone for newly diagnosed patients (4). TMZ which is an oral alkylating agent, has showed antitumor activity in the treatment of glioma (5, 6). The combination of radiation and TMZ therapy prolonged the median survival rate to 14.6 months and became the standard therapy (7). However, the standard therapy showed only a limited effect on GBM patients until now. This is mainly due to the high property of GBM cells to infiltrate the surrounding normal brain tissue, which prevents a complete tumor resection (8). Therefore, new therapeutic strategies for GBM cancer therapy are required.

2. Therapeutic Application of Mesenchymal Stem Cells

MSCs are an excellent candidates for cell therapy because (a) their tumor tropic migratory property and their strong expression of transgenes, allow stem cells to transport and deliver targeted treatment to both infiltrated and metastasized tumors (9, 10); (b) the cells can expand to therapeutic scales in a relatively short time period (11, 12); (c) human trials of MSCs

thus far have revealed no immunogenic reactions to allogeneic versus autologous MSC transplantation (13-15); (d) MSC transplantation is considered safe and has been widely tested in clinical cardiovascular trials (16, 17); and (e) MSCs are highly proliferative *in vitro* culture and can be easily isolated from the bone marrow and adipose tissues of patients (18, 19). In particular, it has been extensively studied that tumor targeting mechanism of MSCs on tumor microenvironment (20-22). Therefore, it can be expected that MSCs can be an effective tools for delivering drug agents to cancer lesions for cancer therapy. Recently, Aboody et al reported that combination therapy with neural stem cells and a suicide gene is effective in mice and those results led to approval for a human trial (23).

3. Suicide Gene Therapy

A promising strategy based on enzyme prodrug therapy is suicide gene therapy such as herpes simplex virus-thymidine kinase/ganciclovir (HVS-TK/GCV) and CD/5-FC (24-27). It was reported that HSV-TK transfected cancer cells could convert GCV to GCV triphosphate, which acts as an inhibitor of DNA synthesis. Moreover, a bystander killing effect on neighboring cancer cells that do not express HVS-TK has been reported (28). Another enzyme/prodrug system that has attracted considerable attention is the CD/5-FC combination. CD, which comes from *E. coli.* can convert prodrug 5-FC into cytotoxic 5-FU. 5-FU is one of the most widely used anti-cancer drugs. The main cytotoxic mechanisms are the inhibition of DNA and RNA synthesis. Metabolites of 5-FU also inhibit thymidylate synthase (TS) activity by the competitive binding of TS (29). It was reported that CD is an attractive suicide gene for gene cancer therapy because

of its stronger anti-cancer effects compare other suicide genes (30, 31). Therefore, tumor specific delivery of the CD gene has been studied extensively (9, 32, 33).

4. Molecular Imaging and its Application

Molecular imaging systems are useful for evaluating the therapeutic efficacy of new therapeutic strategies. Bioluminescence imaging (BLI) is one of the most powerful systems to validate drug efficiency due to its high sensitivity, relatively low cost, efficiency, and versatility, and it is easy to translate small animal studies (34, 35). The luciferase gene (Luc) from the firefly *Photinus pyralis,* is the most commonly used luciferase gene and converts chemical energy into photons.

BLI is simple because a complicated imaging substrate, such as radioisotopes for PET and contrast agents for MRI, is not necessary. BLI is now routinely applied to serially detect the progression and retardation of xenografted tumors in small animal models. However, the disadvantages include the requirement for genetically encoded luciferase, the injection of the substrate to enable light emission, and the dependence of the light signal on tissue depth. These disadvantages make BLI difficult to extend to human studies (36).

Magnetic resonance imaging (MRI) and positron emission tomography (PET) are clinically used for diagnosis and for monitoring therapeutic effects on cancer (37, 38). The advantage of MRI is that gives anatomic image with high resolution and some information about physiology. Therefore, anatomical imaging by MRI is the most widely used method to determine

the target for treatment in brain tumors. However, distinguishing the ‘‘true’’ extension of tumor cells into the adjacent brain regions has been a difficult task, because glioma cells are highly infiltrated into normal brain tissue, particularly in glioblastoma multiforme(39). Moreover, increased enhancement for MR imaging can be induced by a variety of nontumoral processes, such as treatment-related inflammation, ischemia, subacute radiation effects, and radiation necrosis (40, 41)

PET provides biochemical information related to tumor metabolism or the proliferation rate using different tracers. It plays an important role in improving diagnostic procedures in the management of malignant glioma. In brain tumors, [18F] fluorodeoxyglucose (FDG) and 11C-methionine (MET) are the two most widely used tracers. PET with 18F-FDG directly reveals the glucose metabolic activity of tumor cells and is predictive of patient outcomes (42, 43). However, low tumor-to-background ratios due to the high glucose metabolic activity of healthy brain tissue and the variability of glucose uptake in recurrent high-grade gliomas limit the usefulness of 18F-FDG PET (44). 11C-methyl methionine (MET) is the most widely used amino acid for brain tumor evaluation because of an increased amount of amino acid transport and protein synthesis in tumor cells (45-47). Thus 11C-MET scanning appears to be a valuable tool for defining the boundaries of malignant gliomas. Previous PET studies have reported that MET-PET allows earlier and more accurate delineation of tumor extension than anatomical imaging, such as computed tomography or MRI alone (48, 49).

5. Aim of the Study

The main purpose of this study is to monitor the therapeutic effect of CD expressing MSC and prodrug 5-FC in malignant glioma using molecular imaging. In detail, the suicide CD-expressing MSC and 5-FC therapy for glioma was evaluated using various molecular imaging systems (BLI, MRI, PET). Moreover, the relationship between the therapeutic effect of MSC/CDs with 5-FC and the expression levels of 5-FU metabolism related genes in glioma was investigated.

MATERIALS AND METHODS

1. Establishment of reporter gene containing glioma cell

1.1 Glioma cell culture and transfection

Human glioma cell lines (U373, U87MG) were purchased from ATCC (American Type Culture Collection, VA, USA). The glioma cells were maintained in Minimum essential medium (Welgene, MA, USA) containing 10% fetal bovine serum and 1% antibiotic-antimycotic solution (Gibco, NY, USA). Primary glioma cells from a patient (GBM28) were cultured and maintained in DMEM (Welgene, Worcester, MA, USA) containing 10% fetal bovine serum and 1% antibiotic-antimycotic solution (Gibco, NY, USA). The glioma cells were stably transduced with luciferase lentiviral vector system using lipofectamine (Invitrogen, CA, USA). All cells were incubated at 37 ℃ in a humidified atmosphere containing 5% CO_2.

1.2 Glioma cell imaging

Glioma (U87MG/Luc, U373/Luc, GBM28/Luc) concentrations ranging from 1.25 x 10^4 to 3 x 10^5 cells were plated in a 24-well plate and bioluminescence images were captured after addition of D-luciferin (300 μg, Caliper Life Science, MA, USA) to the media. Correlation between cell number per well and bioluminescence intensity were measured by IVIS 100 system. GFP expressions of glioma cells were determined by confocal microscopy using LSM510 META confocal microscope with a 40x magnification (Carl Zeiss Inc., Oberkochen,

Germany). Excitation light was generated by diode and a helium-neon laser. Cells were fixed for 10 min with 3.7% paraformaldehyde (USB, OH, USA), washed with PBS, and mounted with ProLong Gold (Invitrogen, CA, USA).

1.3 Immuno-blot of glioma cells

Glioma cells were lysed in RIPA buffer (Sigma-Aldrich, MI, USA), supplemented with protease inhibitors. Proteins (20 μg) were separated by SDS-PAGE gel electrophoresis and transferred to polyvinylidene difluoride membrane (Millipore, MA, USA). The membranes were incubated with antibodies specific to GFP (1:5000, Cell signaling, Beverly, MA, USA), luciferase (1:5000, Millipore, MA, USA), DPD (1:2000,Cell signaling, Beverly, MA, USA), β-actin (Sigma-Aldrich, MI, USA). Membranes were treated with anti-rabbit-HRP (Cell signaling, MA, USA), anti-mouse-HRP (Invitrogen, CA, USA) secondary antibody. The specific proteins were visualized by chemoluminescence (Roche, IN, USA) according to the manufacturer's protocol.

2. Establishment of suicide and reporter gene containing MSCs

2.1 MSC culture and transfection

Primary human MSCs from iliac crest bone marrow were isolated and cultured as previously reported.(18) The CD gene and imaging reporter genes were stably transfected with lentiviral vector to the human MSCs. Naïve MSCs and gene manipulated MSCs (MSC/CD,

MSC/Luc, MSC/CD-Luc) were cultured in DMEM (Welgene, MA, USA) containing 10% fetal bovine serum and 1% antibiotic-antimycotic solution (Gibco, NY, USA).

2.2 MSC cell imaging

MSC (MSC/Luc, MSC/CD-Luc) concentrations ranging from 1.25 x 10^4 to 3 x 10^5 cells were plated in a 24-well plate and bioluminescence images were captured after addition of D-luciferin (300 μg, Caliper Life Science, MA, USA) to the media. Correlation between cell number per well and bioluminescence intensity were measured by IVIS 100 system. RFP expressions of MSCs were determined by confocal microscopy using LSM510 META confocal microscope with a 40x magnification (Carl Zeiss Inc., Oberkochen, Germany).

2.3 Immuno-blot of MSCs

Lysates of MSC cells were isolated using RIPA buffer (Sigma-Aldrich, MI, USA), supplemented with protease inhibitors. Protein concentrations were measured using a BCA Protein Assay Kit (Pierce Biotech, IL, USA). Proteins (20 μg) were separated by SDS-PAGE gel electrophoresis and transferred to polyvinylidene difluoride membrane (Millipore, MA, USA). The membranes were incubated with antibodies specific to CD (obtained from Aju university), luciferase (Millipore, MA, USA), β-actin (Sigma-Aldrich, MI, USA). Membranes were treated with anti-rabbit-HRP (Cell signaling, MA, USA), anti-mouse-HRP (Invitrogen, CA, USA) secondary antibody. The specific proteins were visualized by chemoluminescence (Roche, IN, USA)

according to the manufacturer's protocol and detected with LAS-3000 system (Fuji Film, Stockholm, Sweden).

2.4 FACS analysis

Naïve MSCs and gene manipulated MSCs were washed with 2% FBS/phosphate-buffered saline (PBS) and incubated at 4℃ for 30 minutes with 5 μl of monoclonal antibody specific for human cluster of differentiation CD 29, CD44, CD105, CD34 and CD45 (BD PharMingen, CA, USA). Control samples were unstained and results were analyzed using FACS Canto II (BD PharMingen, CA, USA).

2.5 *In vitro* suicidal and anticancer effect

To validate the suicide effect of MSC/CD with 5-FC, MSC/Luc and MSC/CD-Luc cells were seeded at a density of $1x10^4$ cells/well in 24 well plates, and increasing concentration of 5-FC (Kolon Life Science, Gyeonggi, Korea) were added after the cells attached. The medium was changed every other day with fresh medium containing 5-FC. After 7 days, bioluminescence images were captured after addition of D-luciferin (300 μg, Califer Life Science, MA, USA) to the media. The viable MSC/Luc and MSC/CD-Luc cells were evaluated by BLI intensity using IVIS 100 system.

2.6 In vitro and in vivo 19F-MRS measurement

MSC and MSC/CD cells ($1x10^5$) were grown in 6 well plates to subconfluence. Cells were then incubated in growth medium containing 1 mM 5-FC (Kolon Life Science, Gyeonggi, Korea). After 24 hours, conditioned mediums were collected and analyzed using 9T (375.567 MHz) Agilent NMR spectrometer (Agilent Technologies, CA, USA). Chemical phantom samples were constructed by diluting of 5-FC (Kolon Life Science, Gyeonggi, Korea) and 5-FU (Sigma-Aldrich, MI, USA) chemical compound. in 10% FBS DMEM (200 uM, 5ml). Spectra were acquired with a single pulse sequence whole region excitation, 11 min scan time (average: 512). The ratio of peak intensities measured using VnmrJ software program.

In vivo 19F MRS experiments were performed at 375.567 MHz in an Agilent NMR spectrometer (Agilent Technologies, CA, USA). MSC/CD cells ($1x10^6$) were xenografted subcutaneous in right flank of Balb/c-nu mice. After administration of the 5-FC (500 mg/kg, i.p), serial 19F NMR spectra were acquired every 8.5 min during 0 to 1.5 h (Total repetition time: 500 ms, Number of averages: 1024, Spectral width: 25 kHz, acquisition size: 2048 point). The chemical shift of the 5-FC resonance was set to 0 p.p.m. The 5-FU signal observed around 1.2 p.p.m. The signal positions were verified with phantom samples of 5-FC and 5-FU (Sigma-Aldrich, MI, USA) in culture medium.

2.7 Migration and in vitro tumor targeting assay

To investigate migration abilities of MSCs, wound healing assay was performed. MSCs were seeding on to 6 well plates. After create a scratch of the cell monolayer, images captured at 0, 4, 8 h after incubation. The distance of migration was measured. To investigate in vitro tumor targeting property of MSCs, Transwell assay was performed using chambers with

polycarbonate inserts (8 μm pore size) (Cell biolabs, CA, USA). The chambers were placed into a 24-well plate. U87MG cells ($1x10^4$) were cultured with 0.5% FBS growth media at the bottom chamber and MSC cells ($1x10^4$) were seeded onto upper chamber of the inserts with 0.5% FBS growth media. After 24 hours of incubation, the number of cells that passed through the inserts was determined using a colorimetric crystal violet assay.

3. Validation of in vitro anticancer effect on glioma cells

3.1 Radiation and TMZ cytotoxic effect on glioma cells

Luciferase expressing glioma cells were seeded in 24 well plates ($1x10^4$) to measure ionizing radiation or TMZ (Sigma-Aldrich, MI, USA) induced cell death. Glioma cells were exposed to ionizing radiation using Cesium-137 irradiator and TMZ at a dose dependently. Four days after, viabilities of glioma cells were measured by quantification of bioluminescence imaging. Bioluminescence intensity was measured by IVIS 100 system.

3.2 5-FU and MSC/CD with 5-FC anticancer effect on glioma cells

To validate the *in vitro* anticancer effect, luciferase expressing glioma cells (U373/Luc, U87MG/Luc, GBM28/Luc) were co-cultured with same ratio of MSC/CD and increasing concentration of 5-FC or different ratio of MSC/CD and 100 μM of 5-FC. After 7 days, 30 μg of D-Luciferin (Caliper Life Science, MA, USA) was added and the viable luciferase expressing

glioma cells were imaged using IVIS 100 system. The intensity of luciferase activity of viable cells were measured and analyzed with IVIS 100 system.

4. Validation of in vivo anticancer effect on xenograft model

4.1 Animal modeling and tumor tropism of MSC/CD-Luc

BALB/c nude mice (male, 6 to 8 weeks old) were used in accordance with Institutional Animal Care and Use Committee of Seoul National University Hospital guidelines. The intracranial xenograft mouse model was constructed as described previously (50). Mouse were anesthetized, and U87MG cells ($3x10^5$ in 4ul PBS) were transplanted into striatum (anteroposterior, +0.5; mediolateral, +1.8; dorsoventral, 3.0) using a stereotaxic device (Stoelting, IL, USA). The cells were injected at a rate of 0.25 ul/min with a 30-guage needle on a 10 ul Hamilton syringe. To evaluate the tumor tropism of MSC, MSC/CD-Luc cells ($3x10^5$) were inoculated into opposite site of tumor lesion 1 week after U87MG cell inoculation. Briefly, mice were anesthetized with isoflurane and the migration of MSC/CD-Luc was monitored once a week by IVIS 100 system.

4.2 Imaging of the therapeutic effect of MSC/CD and 5-FC on orthotopic model

To evaluate the therapeutic effect of MSC/CD and 5-FC, MSC/CD cells ($3x10^5$) were inoculated into tumor lesion from 4 days after U87MG cell ($3x10^5$) inoculation and then 500 mg/kg of 5-FC was injected intraperitoneally 5 days a week. The tumor growth of orthotopic

model was monitored and evaluated using BLI, MRI, PET imaging method. For BLI imaging, D-luciferin (300 μg) was delivered via intraperitoneally injection 10 minutes before imaging of the U87MG/Luc cells in orthotopic model using IVIS imaging system once a week.

Three weeks after U87MG/Luc cell inoculation, the mice were placed in a small animal PET scanner and anesthetized with isoflurane inhalation. 11C-MET was injected intravenously, with a dose of 14 MBq ~ 22.2 MBq per mice. Static images were acquired for 10 min after tracer injection and CT was also performed for attenuation correction. PET/CT images and the SUV values were analyzed by explore Vista-CT software program. All MRIs were acquired by T2-weighted images (turbo-spin echo sequence) using SIMENS 3-tesler scanner with animal 6 channel coil. PET and MRI images were processed and analyzed by Osirix software program.

5. Genetic analysis in glioma cells

5.1 RT-PCR and Real Time PCR

To determine the mRNA expression of 5-FU metabolism related genes on the glioma cells, RT-PCR and real-time PCR were performed. Total RNA was extracted with TRIzol reagent (Invitrogen, CA, USA) according to the manufacturer's protocol. cDNA was synthesized with 1 μg of total RNA using cDNA synthesis master kit (Genedepot, TX, USA). The primer pairs used were showed at Table 1. PCR conditions were 30 sec at 95 ℃ for denaturation, 40 sec at 58 ℃ for primer annealing, 30 sec, 40 sec at 72 ℃ for primer extension. The PCR products were analyzed by 1.2 % agarose gel electrophoresis. Gene expression in DPD was measured by

quantitative RT-PCR using 7700 ABI PRISM sequence detector system (Applied Biosystems, Foster City, CA, USA). PCR primers and fluorogenic probes for DPD genes (Hs00559279_ml), TS (Hs00426591_ml), TP (Hs00157317_ml), OPRT (Hs00923517_ml) and GAPDH genes (Hs99999905_ml) were purchased as Assays-On-Demand (Applied Biosystems, Foster City, CA, USA). Results from qRT-PCR reactions of studied genes were normalized to the Ct values of GAPDH and converted to the fold-change values, relative to the U87MG sample.

5.2 Down-regulation of DPD gene

Non-targeting control siRNA and DPD targeted siRNA were purchased from Santa Cruz Biotechnology (Santa Cruz, TX, USA). U373/Luc cells ($1x10^4$ /well) were cultured in antibiotic-free medium overnight and then transfected with the siRNA for control siRNA (5 nM) or DPD (5 nM), using lipofectamine 2000 (Invitrogen, CA, USA). Seventy two hours later, the transfected cells were washed and used for subsequent experiments. RT-PCR was performed to validate down regulation of DPD genes in U373/Luc cells by DPD siRNA. DPD down-regulated U373/Luc cells were treated with 5-FU for 7 days. Survived cells were imaged and analyzed using IVIS 100 system.

5.3 cDNA Microarray

Total RNA of glioma cells (U8MG, U373, GBM28) was extracted with TRIzol reagent (Invitrogen, CA, USA) according to the manufacturer's protocol. The transcriptional profile of

glioma cells were characterized by oligonucleotide microarray analysis, using MA-human agilent 44K (ebiogen, Seoul, Korea). In order to define DNA expression levels of glioma cells, glioma cells were clustered together by DNA repair related genes (54 genes) and 5-FU metabolism related genes using TIGR Multi-experiment viewer (MeV). Each cluster was determined by hierarchical clustering algorithms with Pearson correlation as similarity measurement of each glioma cells. Hierarchical clustering was performed grouping clusters according to their similarities in gene function representation.

6. Statistical analysis

All experiments were conducted at least in triplicate. Statistically significant differences were determined using the two-paired Student's *t* test. All statistical analysis was performed using Microsoft Excel 2010. $P < 0.05$ was considered significant

.

RESULTS

1. Standard Therapy and 5-FU Therapy for Glioma

1.1 *In vitro* radiation and TMZ cytotoxicity effect on glioma cells

Each glioma cell was stably transduced with luciferase and GFP dual reporter lentiviral vector system (U87MG/Luc, U373/Luc, GBM28/Luc). An immunoblot assay revealed that all glioma cells expressed GFP and luciferase proteins. The glioma cells were visualized by GFP using a confocal microscope imaging system and FACS analysis revealed that over 90% of all glioma cells expressed GFP (Figure 1A~1C). Figure 1D shows that, as the number of glioma cells increase, the bioluminescent intensity increases. The analysis of intensities in the region of interest (ROI) demonstrates a high correlation between the intensity and the number of glioma cells (U373/Luc, R^2:0.9939; U87MG/Luc, R^2:0.994; GBM28/Luc, R^2:0.9923). To investigate the therapeutic efficacy of standard therapy, luciferase expressing glioma cells were treated with ionizing radiation and TMZ. Consequently, the survival rates of all glioma cells decreased with increased doses of radiation. At 3 Gy, the respective percentages of apoptotic cells were 17.2% ± 9.59% (U87MG/Luc), 57.9% ± 6.88%(U373/Luc) and 52.0 ± 6.0%(GBM28/Luc). At 3 and 9 Gy, U87MG/Luc cells showed significant radio-resistance characteristics compared to U373/Luc and GBM28/Luc cells (Figure 2A). When the glioma cells were treated with TMZ, no significant cytotoxic effects on the glioma cells were observed (Figure 2B). These results indicate that current radio-chemotherapy methods cannot effectively suppress glioma cells such as radio-chemo resistant U87MG glioma cells.

cDNA microarray analysis was performed to investigate the different therapeutic response of glioma cells to radiation. Heat-map microarray results revealed that sixteen nuclear excision repair genes (NER, CDKN1A; DDB2; CCNH; ERCC1; CETN2; ERCC5; DUT; TF2H1) and base excision repair genes (BER, TDG; PARP1; PARP3; APEX1; TDP1; MNAT1) showed significantly different expression levels in three glioma cells. In addition, U87MG cells strongly express DNA repair related genes compared to the other glioma cells (Figure 3).

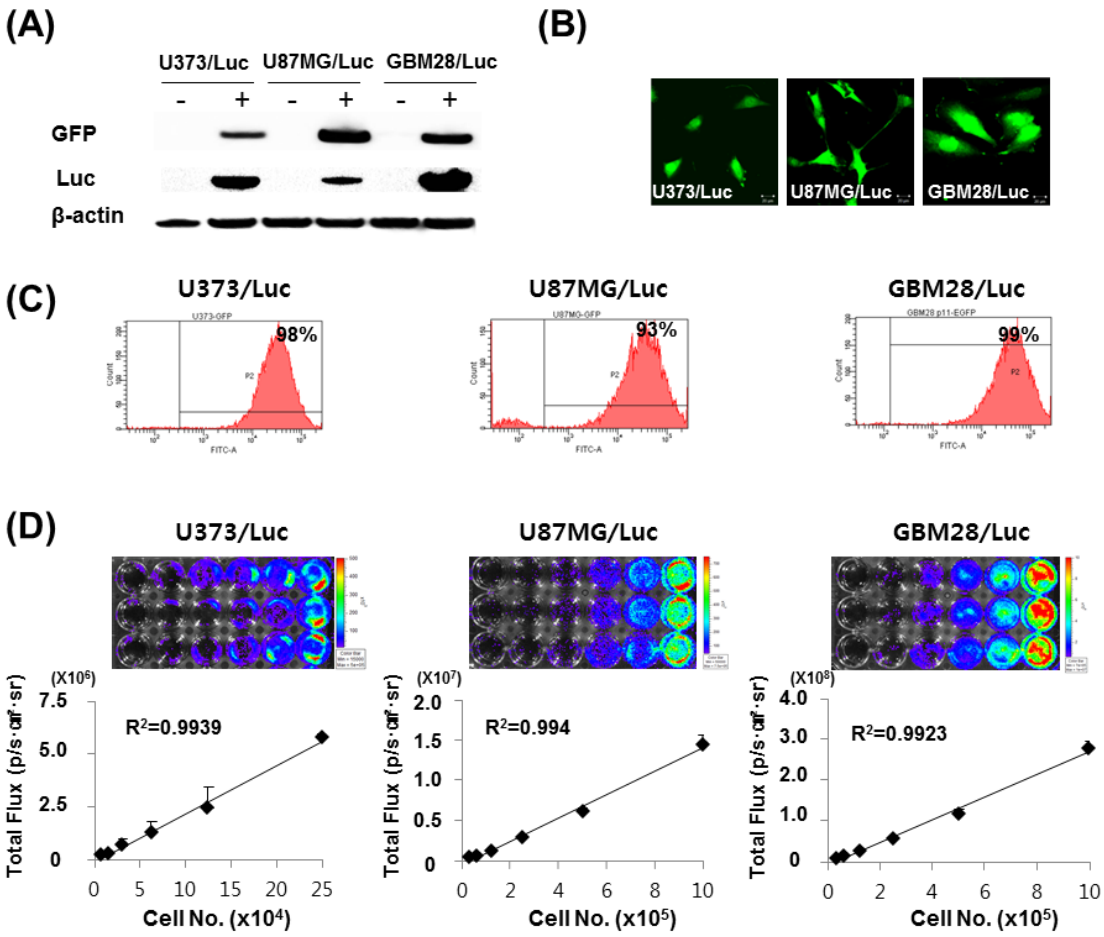

Figure 1. Visualization of GFP and luciferase reporter gene inserted glioma cells

(A) Expression of GFP and luciferase in reporter gene infected glioma cells were determined by Immuno-blotting. All glioma cells expressed GFP and luciferase proteins. (B) Reporter gene infected glioma cells were imaged by green fluorescence with 40x magnifications of confocal microscope. (C) FACS analysis was performed to validate the population of GFP expressing glioma cells. (D) Bioluminescence intensity of glioma cells were imaged and quantified by cell number dependently using IVIS 100 system. Linear regression analysis indicated high correlation between glioma cell number and intensity of ROI (U373/Luc, R^2:0.9939; U87MG/Luc, R^2:0.994; GBM28/Luc, R^2:0.9923). Bars represent mean ± SD.

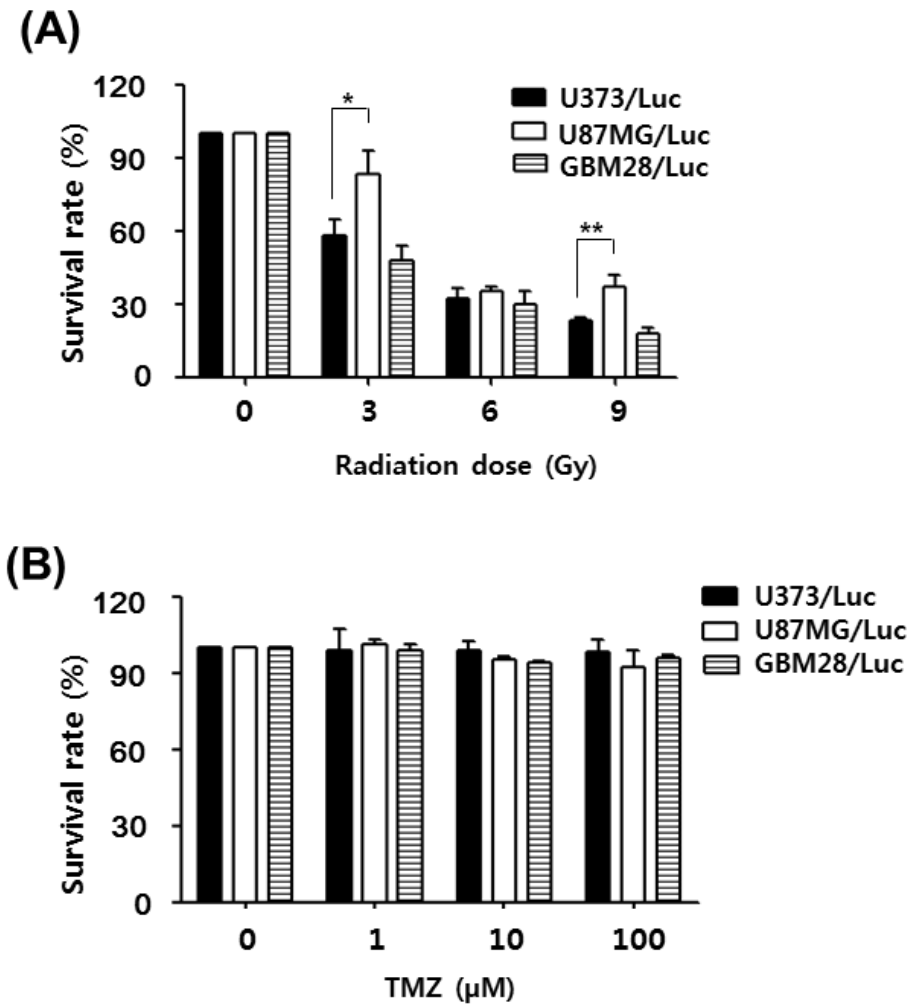

Figure 2. Cytotoxicity of ionizing radiation and TMZ treatment on glioma cells

(A, B) Luciferase expressing glioma cells ($1x10^4$) were seeded on to 24 well plates and treated with indicated dose of (A) ionizing radiation and (B) TMZ. Four days later, bioluminescence intensity of survived cells was measured and analyzed with IVIS 100 system. After radiation, all the glioma cells showed cytotoxicity with increased dose of radiation. U87MG glioma cells showed the most radioresistancy than other glioma cells. There was no cytotoxic effect on all glioma cells after TMZ treatment. Bars represent mean ± SD. (*, $P<0.05$; **, $P<0.01$)

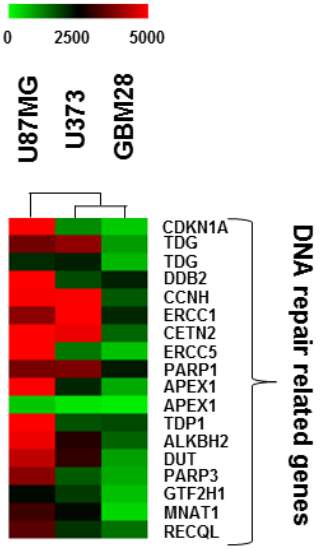

Gene	Description
CDKN1A	cyclin-dependent kinase inhibitor 1A (p21)
TDG	thymine-DNA glycosylase
TDG	thymine-DNA glycosylase
DDB2	damage-specific DNA binding protein 2
CCNH	cyclin H
ERCC1	excision repair cross-complementation group 1
CETN2	centrin 2
ERCC5	excision repair cross-complementation group 5
PARP1	poly (ADP-ribose) polymerase 1
APEX1	APEX nuclease (multifunctional DNA repair enzyme) 1
TDP1	tyrosyl-DNA phosphodiesterase 1
ALKBH2	alkB, alkylation repair homolog 2
DUT	deoxyuridine triphosphatase
PARP3	poly (ADP-ribose) polymerase 3
GTF2H1	general transcription factor IIH, polypeptide 1
MNAT1	MNAT CDK-activating kinase assembly factor 1
RECQL	RecQ helicase-like

Figure 3. Expressions of DNA repair related enzymes in glioma cells

The transcriptional profile of glioma cells were characterized by oligonucleotide microarray analysis, using MA-human agilent 44K. Glioma cells were clustered together by DNA repair related genes using TIGR Multi-experiment viewer (MeV). Each cluster was determined by hierarchical clustering algorithms with Pearson correlation as similarity measurement of each glioma cells. Hierarchical clustering was performed grouping clusters according to their similarities in gene function representation. U87MG showed the strongest expression of DNA repair pathway related genes among the three glioma cells.

1.2 5-FU cytotoxicity and 5-FU metabolism related gene expressions in glioma cells

In order to inhibit DNA synthesis in glioma cells that highly express DNA repair related enzymes, 5-FU cytotoxicity in glioma cells was evaluated. The viability of glioma cells decreased with 5-FU in a dose dependent manner. Interestingly, the therapeutic response of each glioma cell was different. For instance, 13.4% ± 1.69% of U87MG/Luc cells survived after 5-FU treatment (8 uM), while 44.2% ± 9.1% of U373/Luc cells and 21.6% ± 9.1% of GBM28 cells survived (Figure 4). These results indicate that U87MG/Luc cells were two times more sensitive to 5-FU than U373/Luc cells.

Two main action mechanisms have been proposed for 5-FU through its active metabolites (Figure 5A). To determine the cause of the different responses of 5-FU therapy, the expression level of several enzymes that could affect the 5-FU therapy response in glioma was evaluated. cDNA microarray, RT-PCR, qRT-PCR and immunoblot analysis results indicate that the expression level of DPD, which is known as a limiting enzyme of 5-FU showed significant differences compared with other glioma cells. In U373 cell analysis, the DPD genes showed the highest expression levels compare to other glioma cells. On the contrary, U87MG showed the lowest expression levels of the DPD genes (Figure 5B and 6). Hierarchical clustering of 5-FU metabolism related gene expression in glioma cells revealed that the U373 cells that represented the minimum sensitive therapeutic effect showed the most different gene expressions compared with U87MG and GBM28 cells (Figure 5B). In general, these results are

logically consistent with previous results indicating that the U373 cells showed minimum sensitivity to 5-FU cytotoxicity.

1.3 Sensitization of 5-FU by DPD down regulation

The sensitization of tumor cells to 5-FU was investigated after DPD down regulation in glioma cells. RT-PCR results for U373/Luc cells showed that the expression of DPD is suppressed by the DPD siRNA transfection (Figure 7A). 63% ± 1.7% of DPD siRNA transfected U373/Luc cells died after 5-FU (10 uM) treatment, whereas 49% ± 20% of scrambled siRNA transfected U373/Luc cells died. Therefore, when U373/Luc cells were transfected with the DPD siRNA before the indicated doses of 5-FU treatment, the DPD suppressed cells were significantly more sensitive to 5-FU than the scrambled siRNA transfected cells (Figure. 7B).

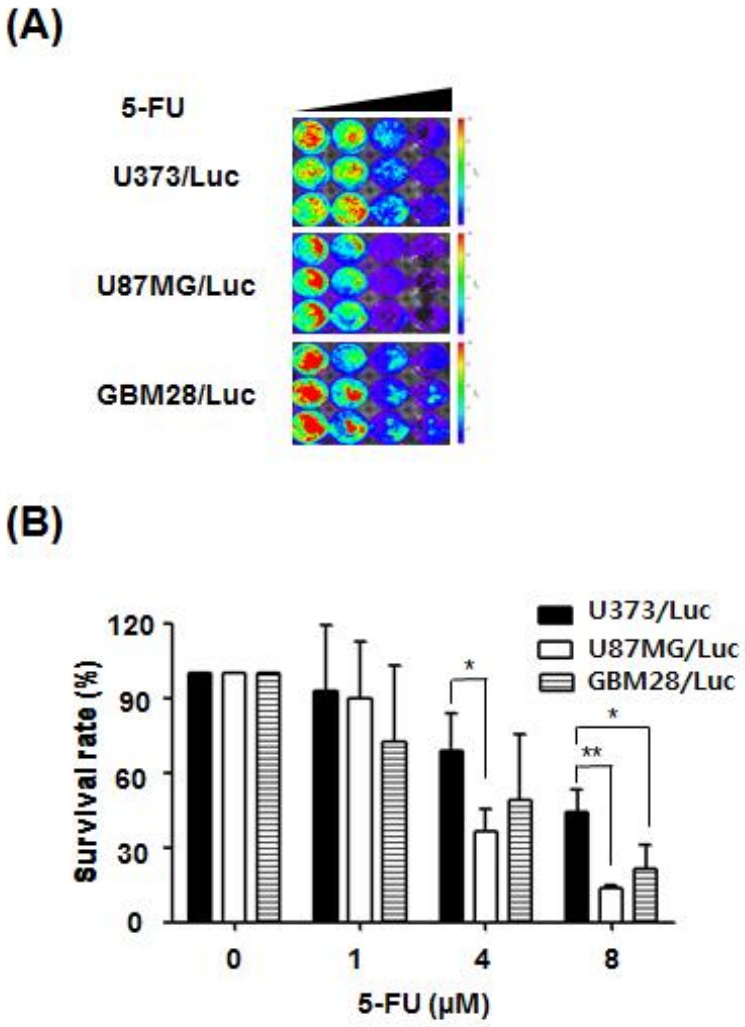

Figure 4. 5-FU cytotoxicity on glioma cells

(A, B) 5-FU cell cytotoxicity assay on glioma cells: (A) Luciferase expressing glioma cells ($1x10^4$) were seeded on to 24 well plates and cultured with increasing dose of 5-FU. Viable glioma cells were imaged by bioluminescence intensity using IVIS 100 imaging system. (B) The intensity of luciferase activity of viable cells were measured and analyzed with IVIS 100 system. U373/Luc showed the least effective response than other glioma cells on 5-FU treatment and U87MG/Luc showed the most sensitive response than other glioma cells. Bars represent mean ± SD. (*, P<0.05; **, P<0.01)

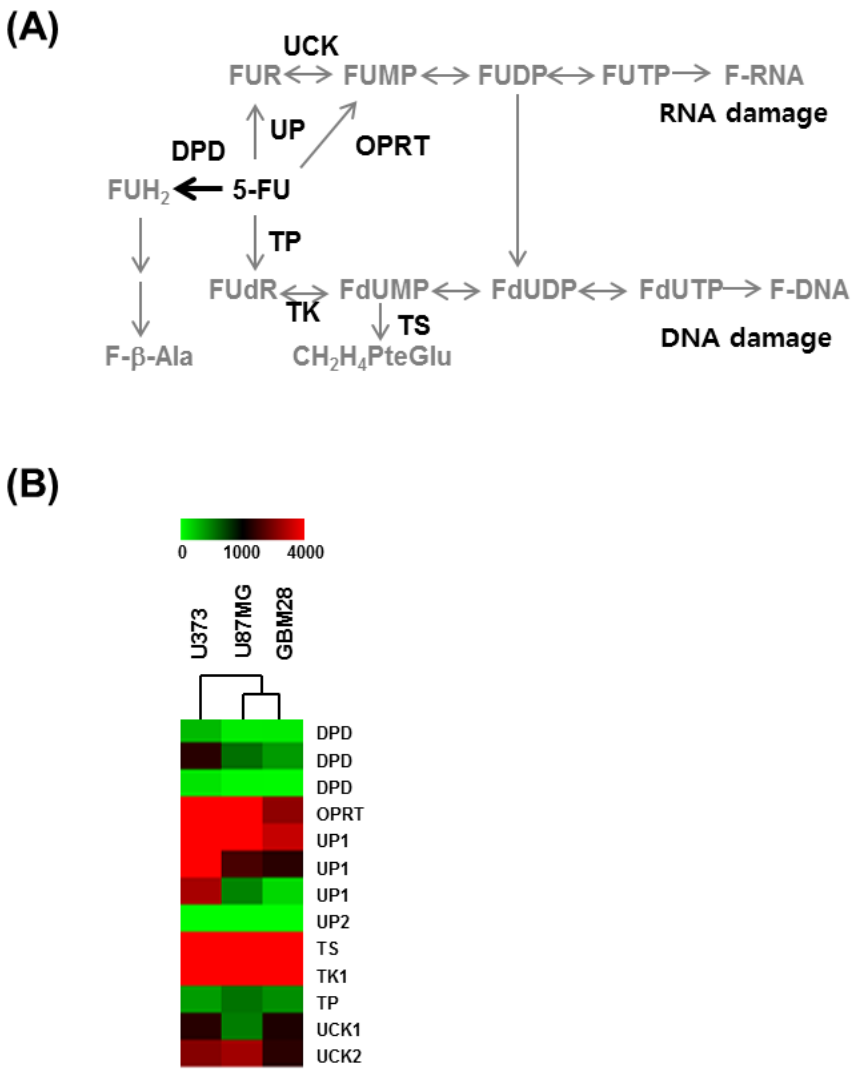

Figure 5. Expression of 5-FU metabolism related enzymes in glioma cells

(A) Schematic diagram show 5-FU metabolic pathway (B) Microarray was performed with glioma cells using MA-Agilent Human 44K v1. Three glioma cells were hierarchical clustered using 5-FU metabolism related gene expression levels. dihydropyrimidine dehydrogenase, DPD; orotate phosphoribosyl transferase, OPRT; thymidylate synthase, TS; thymidine phosphyrylase, TP; uridine-cytidine kinase, UCK; thymidine kinase, TK; 5-fluorodeoxyuridine diphosphate, FdUDP; 5-fluorodeoxyuridine monophosphate, FdUMP; 5-fluorodeoxyuridine, FUdR; 5-fluorouridine diphosphate, FUDP; 5-fluorouridine monophosphate, FUMP; 5-fluorouridine phosphorylase, UP; 5-fluorouridine triphosphate, FUTP; 5-fluorouridine, FUR; deoxythymidine diphosphate, dTDP; deoxythymidine monophosphate, dTMP; deoxythymidine triphosphate, dTTP; fluoro-deoxyuridine triphosphate, FdUTP; 5-fluoro-5,6-dihydrouracil, FUH; α-fluoro-β-alanine, F-β-Ala.

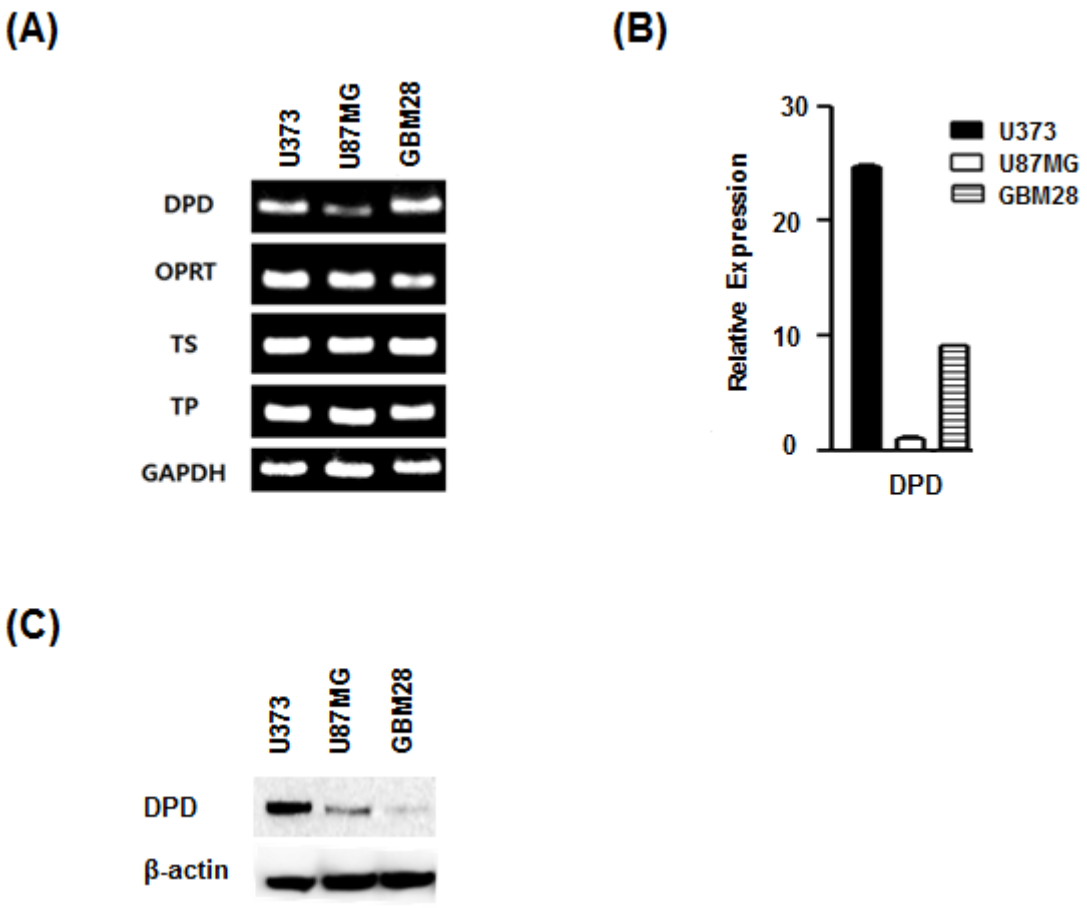

Figure 6. Expression of 5-FU rate limiting enzymes in glioma cells

(A) RT-PCR determined 5-FU related enzyme expression levels in glioma cells. Total RNA was isolated from glioma cells. PCR products were analyzed by 1.2% agarose gel electrophoresis. GAPDH was used as loading control. (B) Real-time PCR and (C) Immuno-blot assay determined DPD expressions in glioma cells. GAPDH and β-actin were used as loading control. Real-Time PCR reactions of studied genes were normalized to the Ct values of GAPDH and converted to the fold-change values, relative to the U87MG sample. U373 cells showed the highest expression levels of DPD genes than other glioma cells.

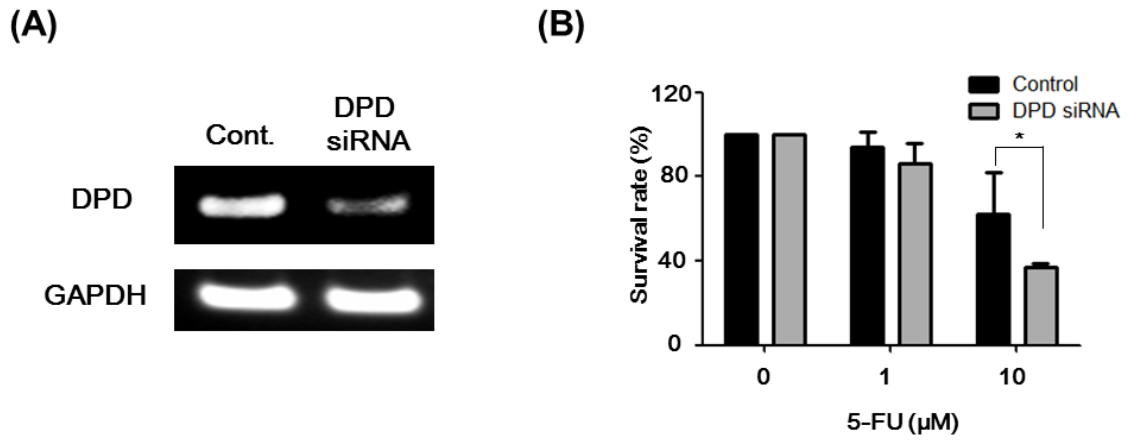

Figure 7. Down regulation of DPD in glioma cells

(A) U373/Luc cells were transfected with the siRNA (5 nM) for control siRNA or DPD using Lipofectamine 2000. PCR products were analyzed by 1.2% agarose gel electrophoresis. RT-PCR determined that expression of DPD in U373/Luc cells was down-regulated by treatment of DPD targeting siRNA. (B) U373/Luc cells ($1x10^4$ /well) were cultured in antibiotic-free medium overnight and then transfected with control or DPD target siRNA. Then, the DPD down regulated U373/Luc cells were treated with indicating dose of 5-FU. Effects of DPD knock down on sensitivity of U373/Luc cells to 5-FU was measured by luciferase intensity of glioma cells. The DPD down-regulated U373/Luc cells were significantly more sensitive to 5-FU than control siRNA transfected U373/Luc cells. Bars represent mean ± SD. (*, $P<0.05$)

2. MSC/CD and 5-FC Prodrug Therapy for Glioma

2.1 Construction of therapeutic MSCs

In order to use gene and cell combined therapy for glioma, CD as a therapeutic gene and imaging reporter genes, including luciferase and tdTomato were stably transfected to the human bone marrow derived MSCs (Figure 8). To determine the original characteristics of MSCs after genetic manipulation, the expression of stem cell markers was analyzed for naive MSCs and MSC/CDs (MSc/Luc, MSC/CD-Luc). All MSCs were uniformly positive for integrin protein CD29, hyaluronate receptor CD44, and endoglin protein CD105, but were negative for hematopoietic progenitor cell marker CD34, and leukocyte common antigen CD45. Gene manipulated MSCs did not show any differences in stem cell marker expression compared to naive MSCs upon FACS analysis (Figure 9). In addition, the wound healing assay and the Transwell migration assay showed that there were no significant changes between naïve MSCs and gene manipulated MSCs (MSC/CD, MSC/CD-Luc) in terms of cell migration and tumor targeting ability (Figure 10A). It was previously reported that there were no significant differences in the capability of adipocytes, osteocytes and chondrocytes to differentiate between naïve MSCs and the therapeutic MSC/CDs used in this study. It was determined that MSCs and MSC/CDs could proliferate up to 10 passages without growth retardation. Moreover, there was no alteration or mutation of normal karyotypes below passage 11 on these MSCs and MSC/CDs (18). These data demonstrate that the CD expressing MSCs maintain the original properties of MSCs even after genetic manipulation.

Next, the tumor targeting properties of MSCs were monitored using a glioma orthotopic model and MSC/CD-Luc. MRI visualized the growth of glioma cells and BLI visualized the localization of MSC/CD-Luc cells. The MSC/CD-Luc cells were visualized at the opposite side of the tumor site after MSC/Cd-Luc inoculation. However, during the fourth week, the BLI showed that more than 50% of MSC/CD-Luc was migrated toward the tumor site (Figure 10B). These results showed that the therapeutic MSCs have tumor targeting abilities.

In this study, MSCs ($1x10^5$) and MSC/CDs ($1x10^5$) cultured media were analyzed by 19F-MRS to validate the conversion of 5-FC to 5-FU. The chemical shift of the fluorine metabolites was only observed in MSC/CD cultured media. Therefore, 19F-MRS experiments determined that only MSC expressing CD could convert prodrug 5-FC into 5-FU (Figure 11A). Moreover, regarding the ratios of 5-FC and 5-FU peak intensities measured using the VnmrJ program, 19F-MRS spectra determined that $1x10^5$ cells of the MSC/CDs converted 5-FC to 5-FU with 16.3% conversion efficiency following a 24-hour reaction. Conversion of 5-FC to 5-FU was also observed after transplantation of MSC/CDs into the flank region of mice. Both 5-FC and 5-FU resonances were observed in the mouse flank region, and the 5-FU peak gradually increased after 5-FC administration (Figure 11B).

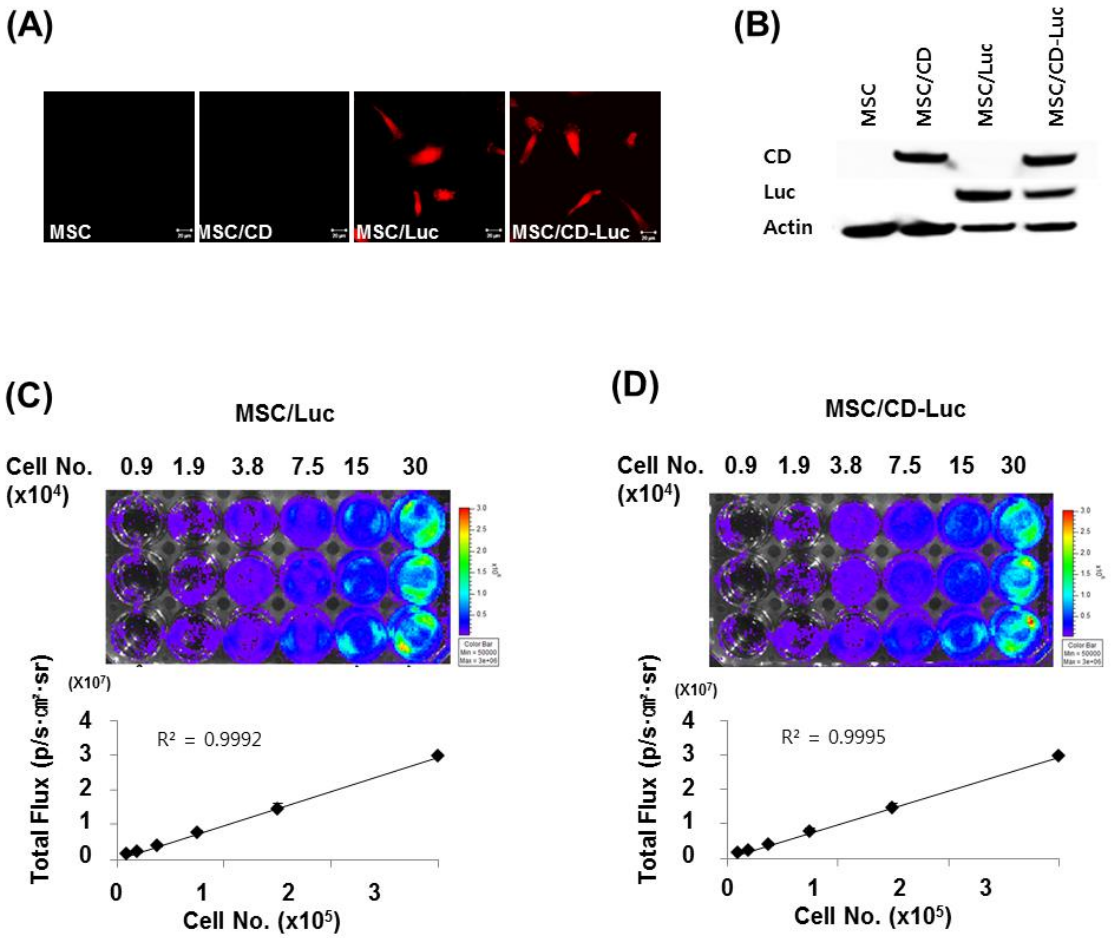

Figure 8. Visualization of RFP and luciferase reporter gene inserted MSCs and MSC/CDs (A) Confocal imaging of MSCs: Reporter gene transfected MSC and MSC/CDs were visualized by red fluorescence using 40x magnifications of confocal fluorescent imaging system. (B) Immuno-blotting determined CD and luciferase expressing in reporter gene infected MSCs. MSC/Luc and MSC/CD-Luc cells were seeded onto 24-well plates at 9 x 10^3 to 3 x 10^4 cells per wells. After incubation for 24 hours, (C) MSC/Luc and (D) MSC/CD-Luc cells were imaged and quantified by cell number dependently using IVIS 100 system. Linear regression analysis indicated high correlation between cell number and intensity of ROI (MSC/Luc, R^2:0.9992; MSC/CD-Luc, R^2:0.9995) Bars represent mean ± SD.

.

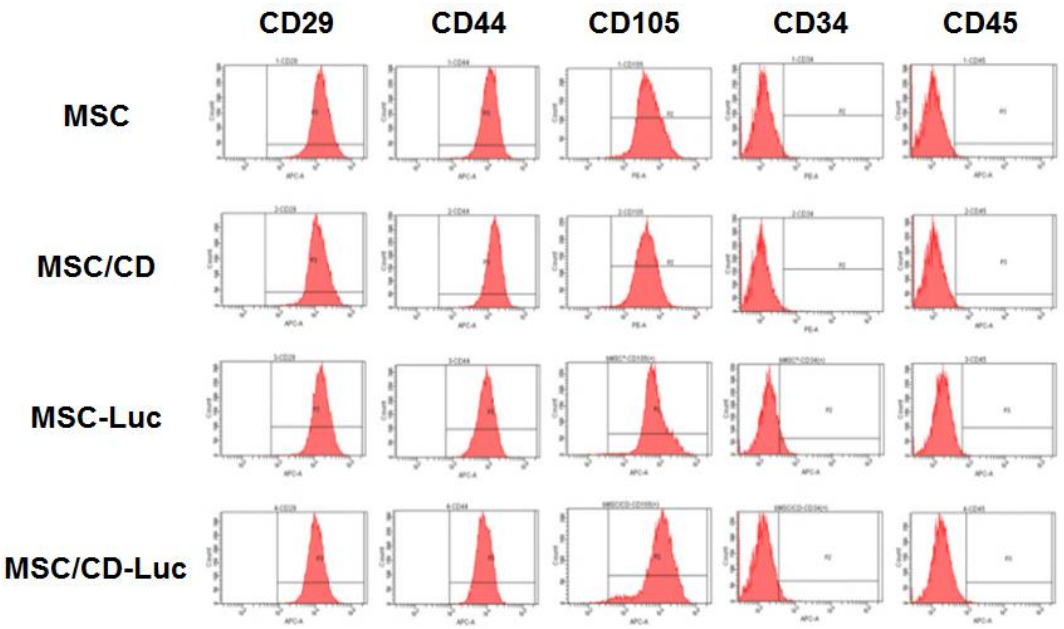

Figure 9. Stem cell marker expression on MSCs

Expression of Stem cell positive (CD29, 44, 105) and negative markers (CD34, 45) were determined on naive MSCs and genetic manipulated MSC/CDs (MSC/Luc, MSC/CD-Luc) by FACS analysis. Naïve MSCs and gene manipulated MSCs were washed with 2% FBS-PBS and incubated at 4℃ for 30 minutes with 5 μl of monoclonal antibodies. Control samples were unstained and results were analyzed using FACS Canto II. There were no differences on stem cell marker expression between gene manipulated MSCs and naive MSCs on FACS analysis. Integrin protein, CD29; hyaluronate receptor, CD44; endoglin protein, CD105; hematopoietic progenitor cell marker, CD34; leukocyte common antigen, CD45

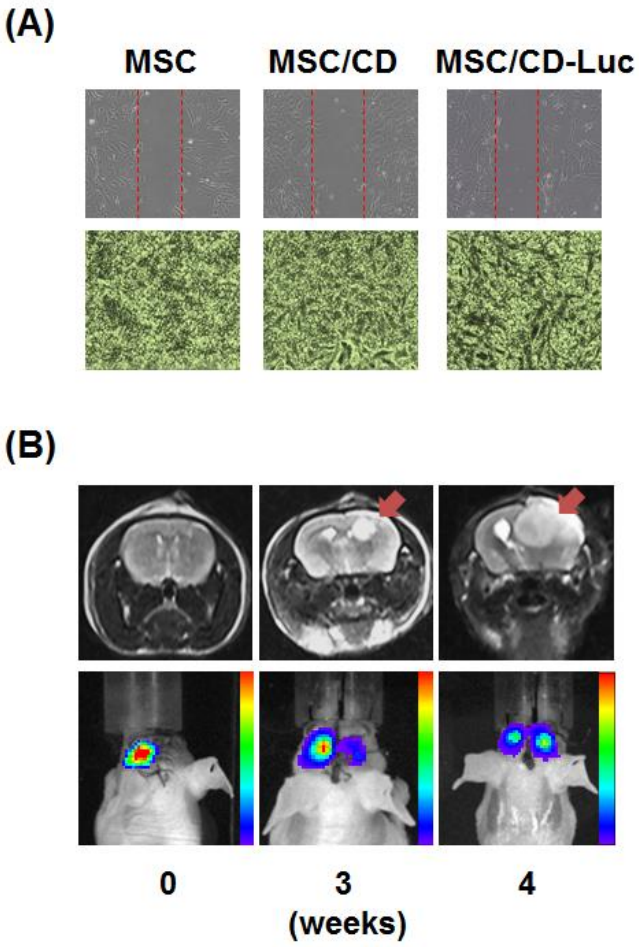

Figure 10. Tumor targeting property of MSC/CDs

(A) Wound healing assay was performed to investigate migration ability of naïve MSC and MSC/CD (MSC/CD-Luc). Migration distance was measured at 0, 4, 8 hours after cells were scratched. Transwell migration system was performed to estimate in vitro tumor targeting ability of MSCs. U87MG cells were cultured in the lower chamber and MSC cells were seeded into the upper chamber. After 24 hours, migrated cells were stained (B) MSC/CD-Luc was transplanted into left striatum of mice 1 week after transplantation of U87MG cells into right striatum of mice. Tumor development (red arrow) and localization of MSCs were monitored using MR and IVIS 100 system. The IVIS imaging demonstrated that more than 50% of MSC/CD-Luc migrated toward the tumor site.

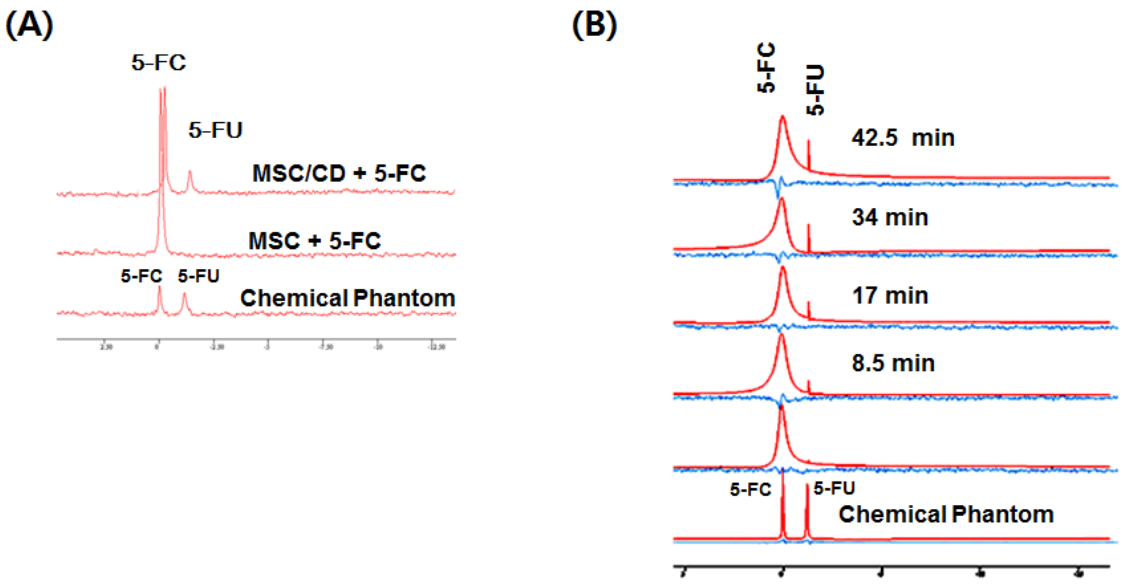

Figure 11. Conversion of 5-FC to 5-FU by MSC/CDs

(A) In vitro 5-FC to 5-FU conversion by MSC/CD was validated using 19F-MRS. MSC ($1x10^5$) and MSC/CD cells ($1x10^5$) were cultured with 1000 uM of 5-FC. After 24 hours, 5-FC and 5-FU in the cultured media was analyzed by 19F-MRS spectra. Chemical compounds of 5-FC and 5-FU were diluted with DMEM media (200 uM, 5ml). 19F-MRS detects the diluted 5-FC and 5-FU as a control (bottom line). The chemical shift of the fluorine metabolites was only detected in MSC/CD cultured media. (B) MSC/CD cells ($1x10^6$) were transplanted into flank region of mouse. 500 mg/kg of 5-FC was transplanted intraperitoneally. 19F-MRS was performed to analyze the conversion of 5-FC to 5-FU half an hour after 5-FC administration. MSC/CD transplanted region of 5-FC and 5-FU were analyzed by 19F-MRS time interval of 8.5 min after 5-FC administration. Spectra were processed using VnmrJ software program. The chemical shift of 5-FC to 5-FU resonances was observed in the mouse flank region, as well as the 5-FU peak gradually increasing after 5-FC administration._

2.2 In vitro anticancer effect of MSC/CDs with 5-FC on glioma cells

The cytotoxic effect of converted 5-FU caused by the MSC/CDs was determined by a viability study of MSC/CD/Luc. As can be seen in Figure 12, the viability of MSC/CD/Luc cells decreased with increasing 5-FC concentrations. At 50 μM of 5-FC, 86.6% of MSC/CDs died. Therefore, MSC/CD/Luc showed cytotoxicity with prodrug 5-FC. In contrast, treatment with 5-FC had no suicidal effect on naïve MSC/Luc. This result determined that the prodrug 5-FC could have cytotoxicity only on cell-expressing CD. A strong correlation (r^2 = 0.9341) was observed between BLI analysis and CCK-8 analysis. There were MSC/CD-Luc signals even after 100 uM of 5-FC treatment. It should be emphasized that CD and reporter genes were co-transfected to MSCs in this experiment. However, it could be possible that a minority of cells was transfected only to reporter genes.

The therapeutic effect of MSC/CDs with 5-FC on luciferase and GFP-expressing glioma cells was estimated based on the luciferase intensity of viable glioma cells. When the therapeutic MSC/CDs were co-cultured with the same number of glioma cells, the viability of the glioma cells decreased with 5-FC concentration in a dose dependent manner. At 50 μM of 5-FC, the survival rate of U373/Luc (34.9%) and U87MG/Luc (17.5%) cells was significantly different (Figure. 13A). In addition, various ratios of MSC/CDs to glioma cells were co-cultured to estimate the therapeutic efficacy of MSC/CDs for glioma cells. Less than 20% of each glioma cells survived (U87MG/Luc: 13.3%, GBM28/Luc: 17.2%) except U373/Luc (41%) cells at 1:3 ratio of MSC/CD to glioma cells (Figure 13B). At a 1:9 ratio of MSC/CDs to glioma cells, only 24%

of U373/Luc cells died, whereas 61.3% of U87MG glioma cells died. These results indicate that U87MG showed the most sensitivity and U373/Luc showed the least sensitivity to MSC/CD and prodrug 5-FC therapy. These MSC/CD and 5-FC prodrug anticancer results correspond to 5-FU therapeutic response and cDNA microarray analysis results of three different glioma cells. The suicidal and therapeutic effects of MSC/CDs and prodrug 5-FC on glioma cells were also visualized by fluorescence imaging. Consequently, it has been observed that when MSC/CD (tdTomato) and glioma cells (GFP) were co-cultured with the same ratio, the growth of 5-FC treated MSC/CDs and glioma cells were suppressed (Figure 14).

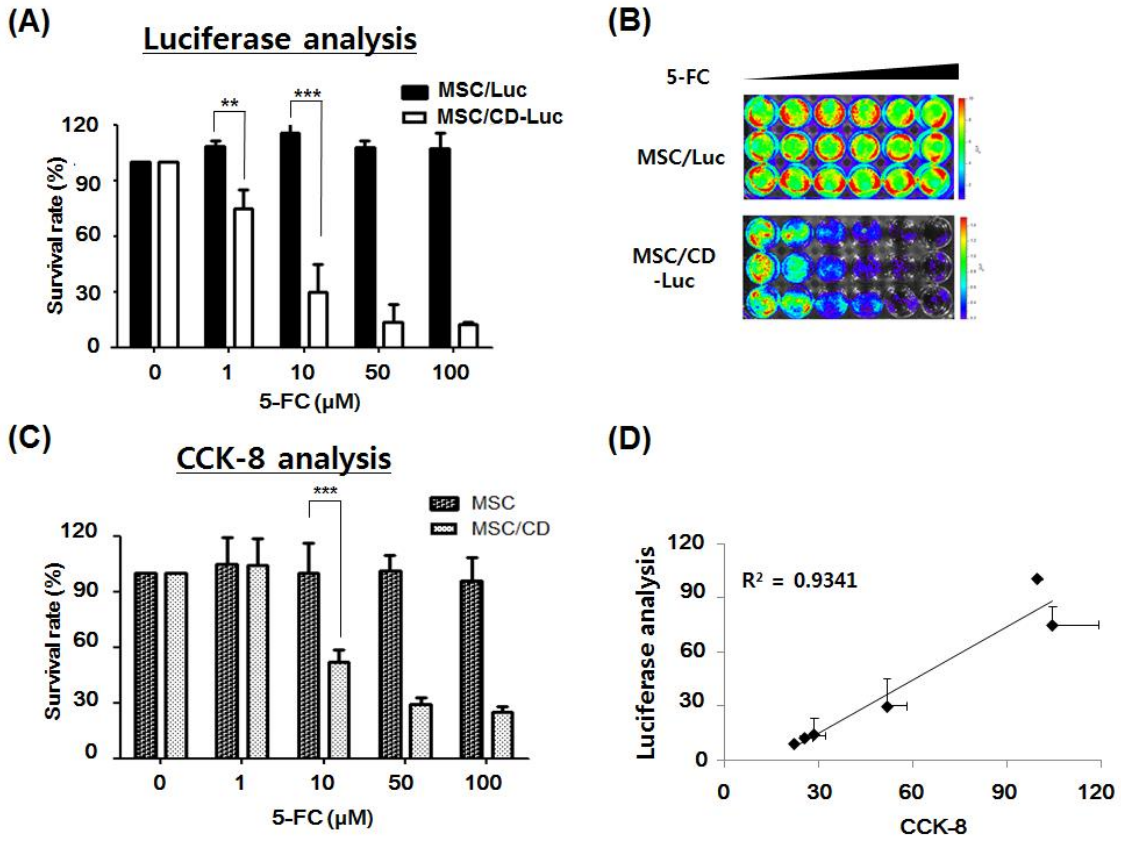

Figure 12. Suicide effect of MSC/CDs

Suicidal effect of MSC/CD was determined by luminescence intensity of viable MSCs. (A, B) MSC/Luc and MSC/CD-Luc were incubated with the indicated concentrations of 5-FC. Seven days later, viable cells were measured by luminescence intensity using IVIS 100 system. (C) CCK-8 analysis was performed to determine the suicidal effect of MSC/CD cells. MSC and MSC/CD cells were cultured with indicate dose of the 5-FC. Seven days later, viable cells were measured by CCK-8 analysis. (D) Correlation between the luciferase analysis and CCK-8 analysis. Cytotoxicity of MSC/CD-Luc was dependent on 5-FC dose. In contrast, there was no suicidal effect on MSC and MSC/Luc after 5-FC treatment. Linear regression analysis indicated high correlation between luciferase analysis and CCK-8 analysis (r^2 = 0.9341). Bars represent mean ± SD. (**, P<0.01; ***, P<0.001)

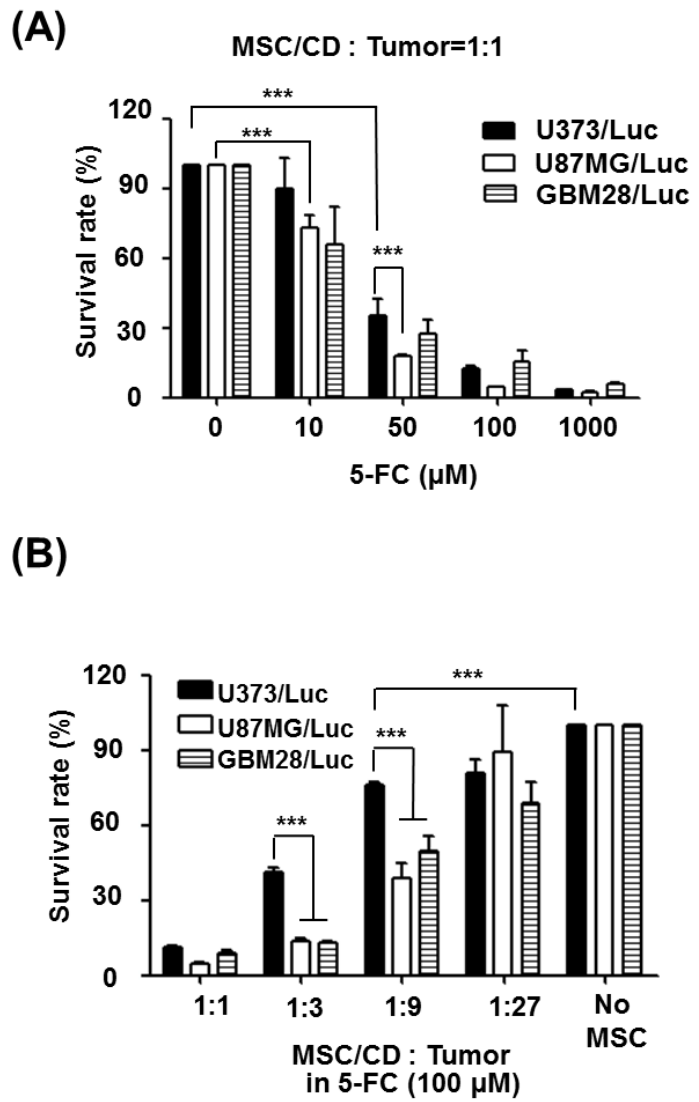

Figure 13. Quantification of the therapeutic effect of MSC/CDs on glioma cells

(A) Luciferase expressing glioma cells ($1x10^4$) were co-cultured with MSC/CD ($1x10^4$) and indicated concentration of 5-FC for 7 days. (B) Different ratio of MSC/CD to glioma cells were co-cultured with 100 μM of 5-FC for 7 days. The viability of co-cultured glioma cells were imaged and quantified by IVIS 100 system. MSC/CD and 5-FC showed anti-cancer effect on glioma cells and had a direct relationship with concentration of prodrug 5-FC and MSC/CD to tumor ratios. Bars represent mean ± SD. (**, P<0.01; ***, P<0.001)

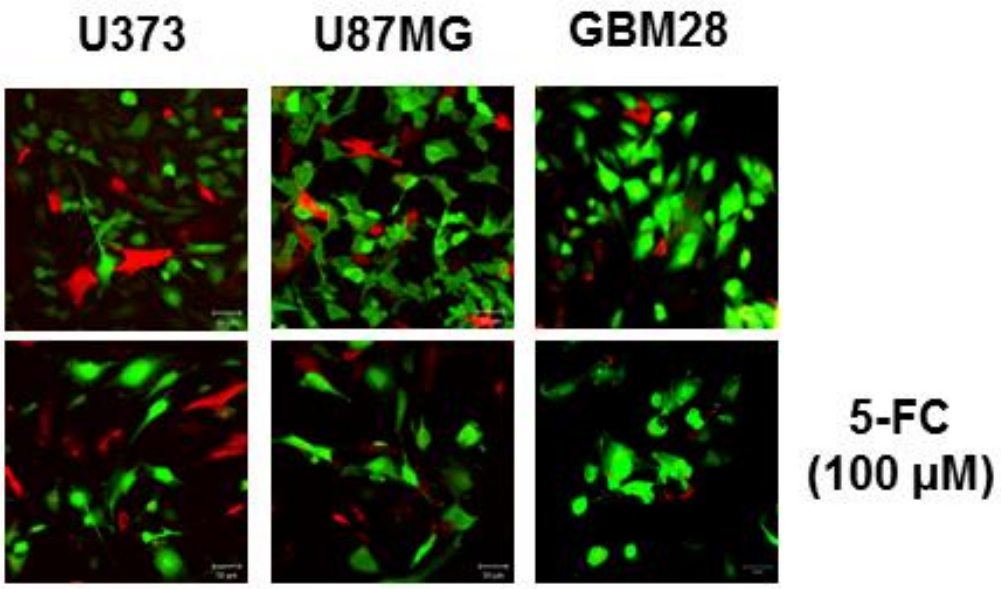

Figure 14. Confocal imaging of the therapeutic effect of MSC/CDs

GFP expressing glioma cells ($1x10^4$) were co-cultured with RFP expressing MSC/CD ($1x10^4$) and 100 µM of 5-FC for 7 days. Glioma cells (GFP) and MSC/CD cells (tdTomato) were visualized by 40x magnifications of confocal microscope.

2.3 Monitoring the therapeutic effect of MSC/CDs and 5-FC on a glioma orthotopic model

The therapeutic effect of MSC/CDs and prodrug 5-FC against a pre-existing U87MG/Luc glioma model was monitored using BLI, MRI, and 11C-MET PET. The imaging modalities visualized that the growth of glioma cells was dramatically suppressed by MSC/CD and 5-FC therapy (Figure 15A-C). Tumor development in each mouse was analyzed using bioluminescence intensity. The MSC/CD and prodrug 5-FC treated group showed 77.9% tumor suppression in comparison to the control group. Tumor volume analysis by MRI revealed that MSC/CD and prodrug 5-FC therapy was able to suppress 72.7% of tumor growth. In addition, value of SUV_{mean} by 11C-MET PET determined 70.1% of the tumor suppression by MSC/CD and prodrug 5-FC treatment. (Figure 15D-F). In this study, BLI analysis is used to determine the proliferation of glioma cells. The quantification of BLI analysis results demonstrated the highest therapeutic efficacy of MSC/CDs and 5-FC. PET/MRI imaging demonstrated that the anatomic tumor lesion and the physiologic tumor lesion were not exactly identical. Therefore, both MRI and PET imaging are needed to accurately evaluate the therapeutic effect. Additionally, Kaplan-Meier survival analysis revealed the prolongation of survival in the MSC/CD therapy group compared with the control group (Figure 16). Taken together, these results indicate that tumor growth was effectively suppressed by MSC/CD and 5-FC therapy.

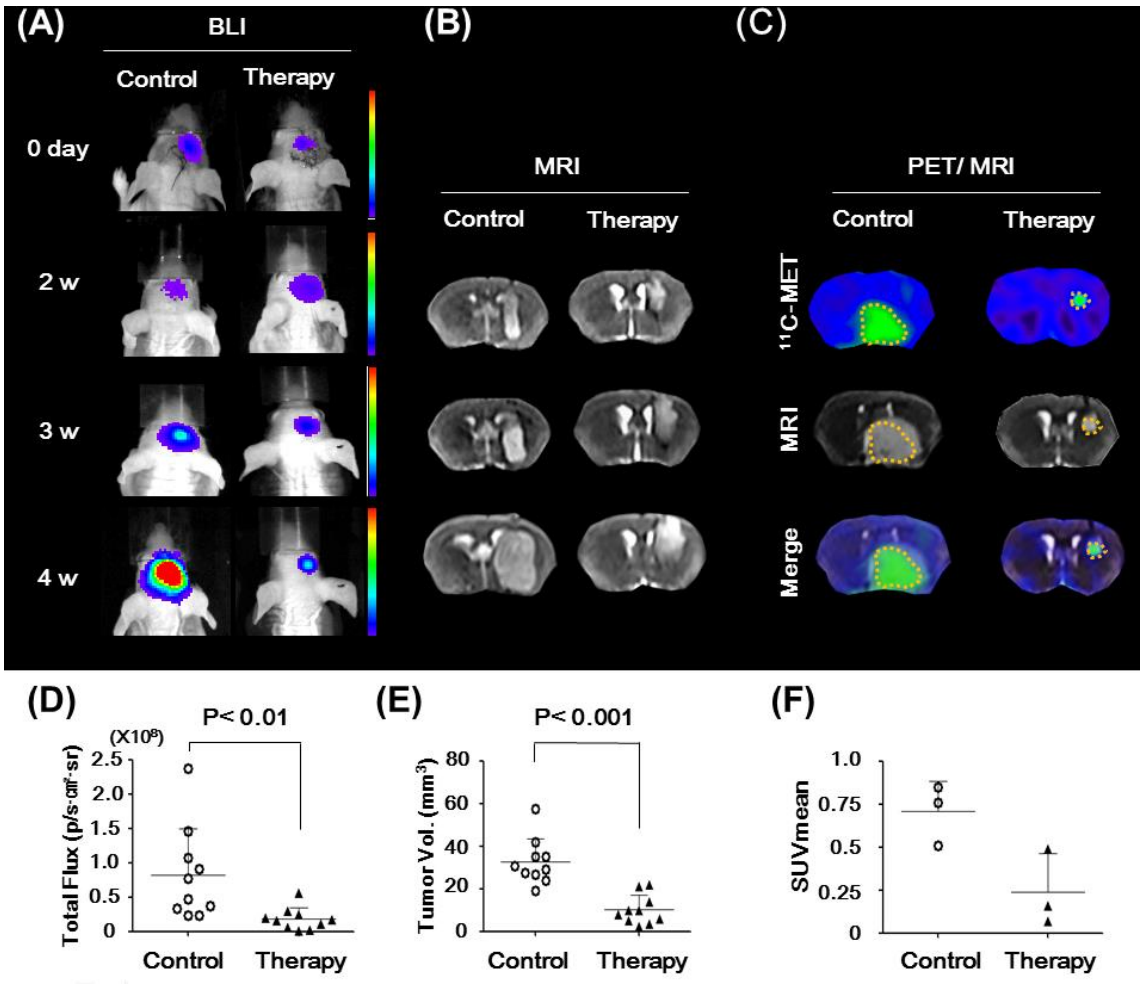

Figure 15. Monitoring the therapeutic effect of MSC/CDs and 5-FC on glioma orthotopic model

U87MG cells ($3x10^5$ in 4ul PBS) were transplanted into mice striatum (anteroposterior, +0.5 mm; mediolateral, +1.8 mm; dorsoventral, 3.0 mm) to construct brain orthotopic model. MSC/CD cells ($3x10^5$) were inoculated into tumor lesion from 4 days after U87MG cell ($3x10^5$) inoculation and then 500 mg/kg of 5-FC was injected intraperitoneally 5 days a week. Tumor growth of U87MG/Luc inoculated orthotopic mouse models were imaged by (A) BLI, (B) MRI, (C) PET (11C-MET). PET and MR images were fused with Osirix software. Tumor cell growth was evaluated by (D) luciferase intensity, (E) tumor volume (F) SUV_{mean}. Quantification of tumor development using molecular imaging revealed that about 70% of tumor growth was suppressed by MSC/CD and prodrug 5-FC therapy

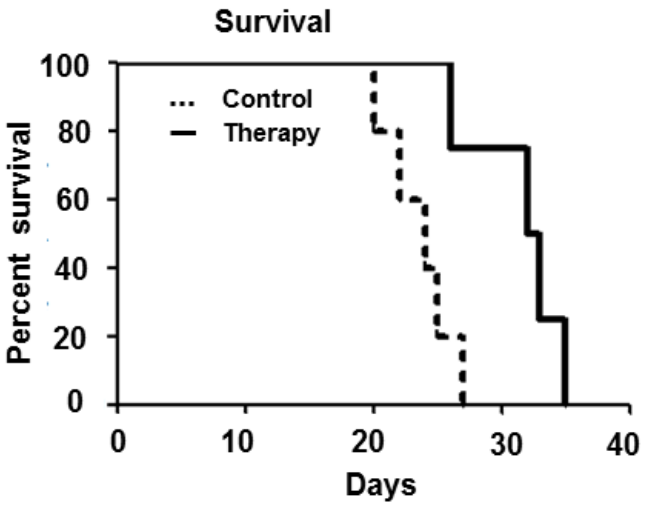

Figure 16. Kaplan-Meier survival curve

The survival of orthotopic mice was analyzed by a log-rank test based on the Kaplan-Meier survival method. Control groups (n=7) were only treated with 5-FC (500 mg/kg) and Therapy groups (n=8) were treated with MSC/CD and prodrug 5-FC (500 mg/kg). The MSC/CD and prodrug 5-FC treated group improved the survival of orthotopic model.

2.4 Safety test of therapeutic MSCs

The proliferation of MSC/CDs was monitored using BLI after the subcutaneous transplantation of MSC/CD-Luc into mice. There were no increasing luciferase signals of MSC/CD-Luc for 24 weeks (Figure 17). In an Immuno-histochemistry (IHC) study, Ki-67 was unstained at the MSC/CD transplantation site 24 weeks after MSC/CD-Luc transplantation. This study determined that there was no development of tumorigenic cells until 24 weeks after MSC/CD-Luc transplantation. In addition, when MSC/CDs were inoculated with glioma cells, there were no significant differences in tumor growth (Figure 18). Therefore, these results indicate that therapeutic MSCs could be safe to use as cell therapy agents.

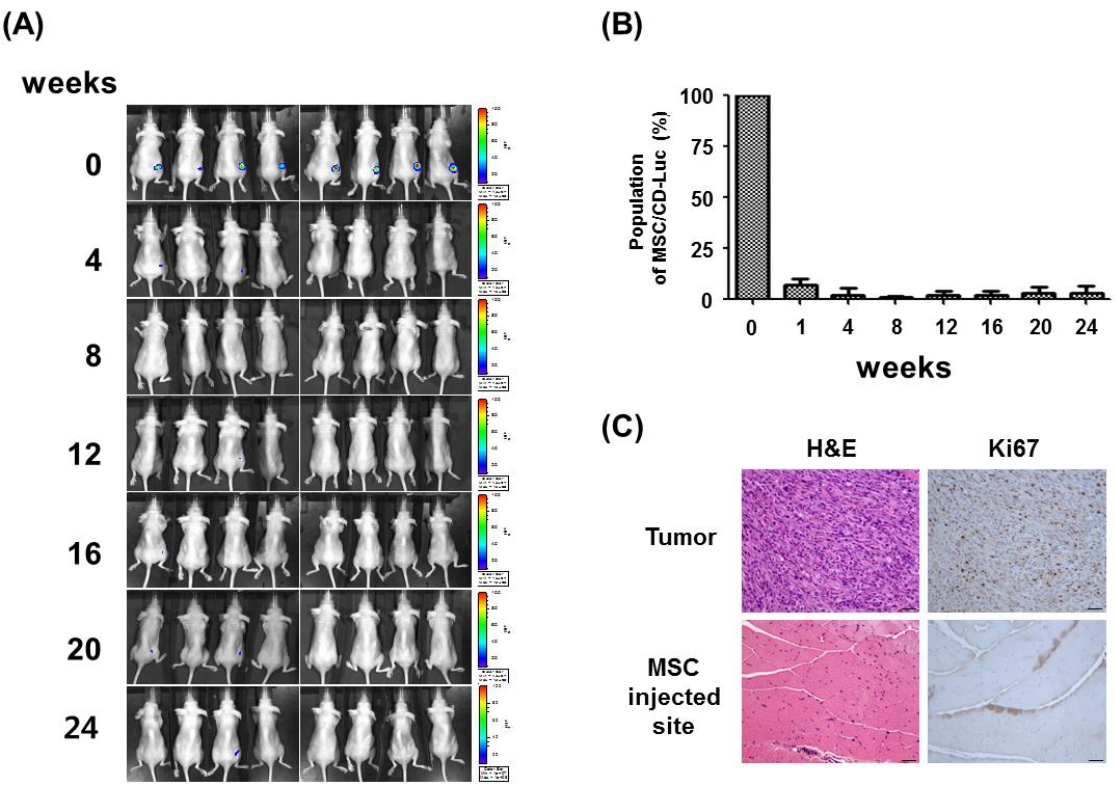

Figure 17. Tumorigenesis of MSC/CDs

(A) MSC/CD-Luc cells were transplanted into right flank of mouse. Localization and proliferation of MSC/CD-Luc cells was imaged by IVIS every 4 weeks for 24 weeks. (B) The survived MSC/CD-Luc cells were monitored and evaluated with luciferase intensity. There were no increasing luciferase signals of MSC/CD-Luc (C) H&E-stained tumor sections from U87MG glioma-bearing mice (Ki67 positive control) and MSC injected site from MSC/CD-Luc transplantation mice. IHC with antibodies against Ki67 revealed tumor cell proliferation. Ki-67 was only stained in tumor tissue.

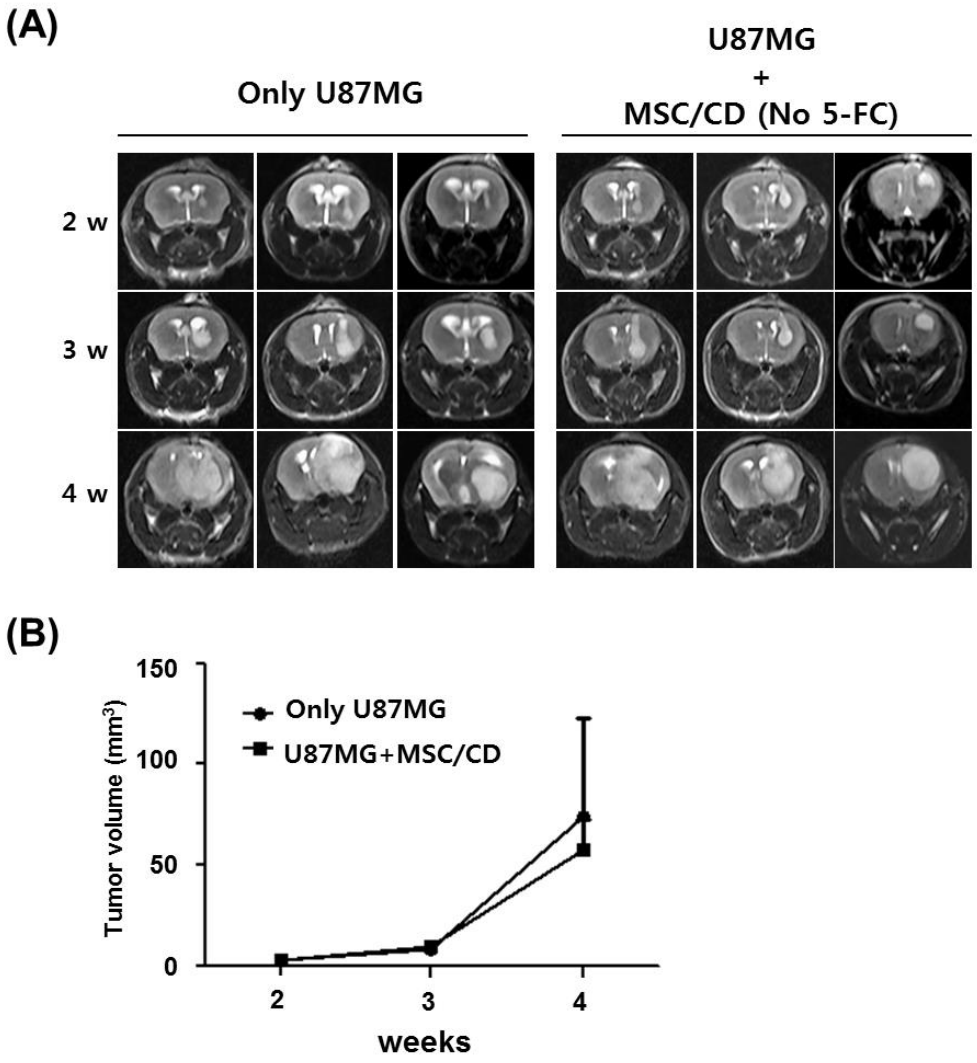

Figure 18. Effect of MSC/CDs on tumor growth

U87MG cells ($3x10^5$ in 4ul PBS) were transplanted into mice striatum to construct brain orthotopic model. MSC/CD cells ($3x10^5$) were inoculated into tumor lesion without 5-FC treatment from 7 days after U87MG cell ($3x10^5$) inoculation. (A) Tumor growth of glioma orthotopic mouse model was imaged by MRI at 2, 3, 4 weeks after U87MG and MSC/CD inoculation. MRIs were acquired by T2-weighted images using SIMENS 3-tesler scanner with animal 6 channel coil. (B) The volume of tumor growth was measured using Osirix software. There were no significant differences in tumor development between control and MSC/CD treated group.

DISCUSSION

GBM is known as one of the most difficult cancers to cure because it is highly malignant and invasive. Infiltrated GBM cells surrounding normal brain tissue are especially difficult to surgically remove. To prevent tumor recurrence, radiation and chemotherapy are used. However, there has been no proper method to treat recurring glioblastoma after tumor surgery and radio-chemotherapy until now. Therefore, tumor targeting therapy methods to kill infiltrated tumor cells in normal brain tissue are needed.

There is growing evidence that MSCs have the ability to migrate to tumors and injury sites (51-53). The molecular factors of involved in MSC migration to tumors has been revealed as a stromal cell derived factor-1(SDF-1), platelet-derived growth factor-AB (PDGF-AB), and CCR families, etc. In particular, it was demonstrated that SDF-1 is one of the major chemokines secreted by MSCs when exposed to a tumor microenvironment. Subsequently, SDF-1 binds to its cognate receptors CXCR4/7 of MSCs to activate Jak2/STAT3 and ERK1/2 signaling, which in turn regulates FAKs that induce the reorganization of the actin cytoskeleton, thereby promoting MSC migration (20-22). In this study, the tumor targeting ability of therapeutic MSCs was non-invasively monitored using BLI in an orthotopic glioma model (Figure 10B). The results showed that more than half of the MSCs migrated toward the tumor lesion. Therefore, MSCs could be expected to easily migrate to surrounding tumor cells and MSC therapy could be an efficient tumor targeting therapy for those infiltrated glioma cells.

In the last decades, cell-based approaches have been extensively investigated for cancer therapy. There are several therapeutic genes such as IL-12 and TRAIL (24-27). However, one problems of with these strategies for clinical application is that the genetically manipulated cells remain in the patient after therapy. To overcome this problem, suicide gene strategies such as HSV-TK/GCV and CD/5-FC, have received considerable attention for their effective anticancer abilities. Suicide gene therapy using gene coding for an enzyme that converts a nontoxic prodrug into a lethal compound is inserted into the tumor cells or tumor targeting agents. In this study, I discussed the conversion of prodrug 5-FC to cytotoxic 5-FU by CD expressing MSCs. In addition, MSC/CDs effectively enhanced not only the anticancer effect on glioma cells but also the suicide when 5-FC was treated (Figure 12, 15). This means that this therapeutic strategy can avoid the risk of genetically manipulated cells in clinical applications by using CD because the therapeutic cells are drained as a result of the suicide effect. Moreover, 5-FU not only induces DNA and RNA damage by the insertion of 5-FU metabolites but also inhibits the TS activity by the competitive binding of TS (29).

TS is an enzyme that catalyzes the conversion of deoxyuridine monophosphate (dUMP) to deoxythymidine monophosphate (dTMP). dTMP is nucleotide that forms thymine. With the inhibition of TS, DNA damage was induced by increasing levels of dUTP and an imbalance of deoxynucleotides. For this reason, TS has become an important target for cancer treatment by means of chemotherapy (54). CD/5-FC showed more therapeutic advantages compared to HSV-TK and other available prodrug therapy methods. In addition it is reported that the ionizing

radiation response increases when ionizing radiation is combined with 5-FU (55). Therefore, a 5-FC/CD system can be used as a radio-sensitizer.

Magnetic resonance spectroscopy (MRS) is a noninvasive diagnostic tool for measuring biochemical changes *in vivo*. Each biochemical, or metabolite, has a different peak in the spectrum that appears at a known frequency. Using this method, several different metabolites, or products of metabolism (amino acids, lipid, lactate, alanine, N-acetyl aspartate, choline… etc) can be detected (56). 5-FC and 5-FU compounds can be monitored using fluorine (19F) MRS (57).

MR images of patients provide precise anatomical information about cancer but this is not sufficient for cancer diagnosis. There are many clinical reports about the pseudo-response and pseudo-progression of GBM on MRI analysis (58-60). Therefore, several imaging parameters are used for glioma diagnosis. The functional and metabolic activity of glioma can be imaged using PET with 18F-FDG, 11C-MET, and 18F-FLT. 18F-FDG shows glucose consumption that could indicate viability of tumor cells. However, it is difficult to image the tumor lesion specifically because of variable background uptake in the normal brain tissue (61). Glioma images with 11C-MET as the amino acid tracer show high sensitivity and specificity (62). However, PET images have the limitation of identifying anatomic information about the body and the morphologies of tumors. Morphologic, functional and metabolic molecular imaging is necessary for diagnosis and to evaluate the therapeutic effects of intracranial primary tumors. Therefore, it is necessary to analyze both PET images and MR images for cancer diagnosis and

to evaluate any therapeutic effects (63, 64). In this research, the PET image was merged with MR image using the Osirix software program. These merged images provide the co-localization of biologic and precise anatomic information of glioma (Figure 15). The value of SUV_{mean} is used to diagnose cancer on PET scans (65). An analysis of PET images showed that the value of SUV_{mean} was much higher in the non-treated orthotopic model than in the MSC/CDs and 5-FC treated orthotopic model. Like the analysis of PET images, the analysis of MR images showed that tumor growth was suppressed by treatment with MSC/CDs and 5-FC compared to the non-treated orthotopic model. Tumor growth analysis using luciferase intensity analysis was similar with tumor volume analysis from the MRI and SUV_{mean} analysis from 11C-MET PET. It is difficult to expect that BLI can be extended to human studies even though it is evident that BLI is a convenient and accurate method for monitoring the therapeutic effect of cancer in small animal models.

Many current cancer therapy agents target the integrity of cellular DNA, which is important to cell survival. These agents induce DNA damage by breaking DNA, forming cross links and targeting DNA-related proteins (66). Ionizing radiation generates oxidative DNA damage by generating reactive oxygen species (ROS) and results in single-strand and double-strand breaks in the double helix. Intracellular nucleotide excision repair (NER) and base excision repair (BER) systems are activated after DNA damage to repair breaks in the double helix. For this reason, the enhancement of DNA repair pathway (NER, BER) related genes is one of the crucial mechanisms causing cellular resistance to DNA-damaging agents (67, 68).

Therefore, the expression levels of DNA-repair related enzymes in glioma cells were analyzed to reveal the reason for radio-resistance in glioma cells. To analyze the expression levels of DNA repair enzymes in glioma cells, 54 DNA repair related genes were studied using a microarray. Glioma cells were clustered together by DNA repair related genes using a TIGR multi-experiment viewer (MeV). Each cluster was determined by hierarchical clustering algorithms with a Pearson correlation as a similarity measurement for each glioma cell. Hierarchical clustering was performed grouping clusters according to their similarities in gene function representation.

In this research, U87MG cells showed more radio-resistance than other glioma cells (U373, GBM28). And I also determined that the radio-resistance of U87MG cells was due to the high expression of DNA repair related genes in those U87MG cells (Figure. 4). Interestingly, the radio-resistant U87MG cells were more sensitive to 5-FU therapy than were the U373 cells (Figure 4). The expression of 5-FU metabolism enzymes, such as DPD, TS, TP, and OPRT, has been estimated in order to predict 5-FU sensitivity in various cancers (69). A microarray analysis found that the sensitivity of 5-FU therapy was due to the expression of 5-FU metabolism related genes in glioma cells (Figure 5). DPD is especially important in MSC/CDs and 5-FC therapy, because it degrades 5-FU into F-β-alanin (70). Of all the gliima cells, U87MG cells were the least expressed cells in DPD in this study. This is why U87MG cells showed the greatest response to 5-FU therapy. The microarray results were closely correlated with the therapeutic effect when glioma cells were clustered by 5-FU metabolism related enzymes. Consistent with in vitro 5-FU therapy results, U87MG cells showed the most sensitive cytotoxicity to MSC/CD

and 5-FC therapy (Figure 14). These results indicate that the gene analysis of glioma cells of patients can predict the efficacy of MSC/CD and 5-FC therapy. When the expression level of 5-FU rate limiting enzymes is low, MSC/CDs and 5-FC therapy can be an option for glioma therapy. Personalized cancer therapy has been proposed and widely studied as the new targeted therapy for cancer patients, because the expression levels of oncogenes and drug metabolism related genes in cancer patients are different (71).

5-FU is an antimetabolite that kills rapidly proliferating cells by inhibiting DNA synthesis. Therefore, the 5-FU converted from 5-FC by MSC/CDs could have a more cytotoxic effect on malignant brain tumor cells compared to MSCs. In an *in vitro* experiment, MSCs showed no reduced survival rate even after high-dose 5-FC treatment (Figure. 13). In addition, in the *in vivo* experiments, the control and therapy groups were treated with the same dose of 5-FC (500 mg/Kg). Only the therapeutic group showed dramatically reduced glioma development. Also, when the MSC/CDs were treated using a glioma orthotopic model without 5-FC, there were no considerable differences in tumor development between the control group and the MSC/CD-treated group (Figure 18). These results indicate that both MSC/CDs and 5-FC are needed for tumor suppression.

Some of the limitations of this research include the need for further study of the effect of bone marrow derived MSCs on brain tissue, the mechanisms of the MSCs migrating towards tumor lesions, and the distribution volume of 5-FU *in vivo* due to MSC/CDs.

In conclusion, I show the therapeutic effect of MSC/CDs and 5-FC on glioma cells *in vitro* and *in vivo* using molecular imaging. A co-culture of MSC/CDs and glioma cells showed a therapeutic effect dependent on 5-FC concentration and the MSC/CD to tumor ratio. Furthermore, the therapeutic effect was closely related with the expression of 5-FU metabolism related enzymes on glioma cells. These promising results demonstrate that therapeutic MSCs and 5-FC are valuable for glioma therapy and show low expression of 5-FU rate limiting enzymes. This research proposes a cancer-targeting therapeutic method to treat tumor cells that have infiltrated or micro-metastasized in normal tissues

REFERENCES

1. Galldiks N, Ullrich R, Schroeter M, Fink GR, Kracht LW. Imaging biological activity of a glioblastoma treated with an individual patient-tailored, experimental therapy regimen. Journal of neuro-oncology. 2009 Jul;93(3):425-30. PubMed PMID: 19183853. Pubmed Central PMCID: 2758365.

2. Viel T, Talasila KM, Monfared P, Wang J, Jikeli JF, Waerzeggers Y, et al. Analysis of the growth dynamics of angiogenesis-dependent and -independent experimental glioblastomas by multimodal small-animal PET and MRI. Journal of nuclear medicine : official publication, Society of Nuclear Medicine. 2012 Jul;53(7):1135-45. PubMed PMID: 22689925.

3. Buckner JC. Factors influencing survival in high-grade gliomas. Seminars in oncology. 2003 Dec;30(6 Suppl 19):10-4. PubMed PMID: 14765378.

4. Stupp R, Mason WP, van den Bent MJ, Weller M, Fisher B, Taphoorn MJ, et al. Radiotherapy plus concomitant and adjuvant temozolomide for glioblastoma. The New England journal of medicine. 2005 Mar 10;352(10):987-96. PubMed PMID: 15758009.

5. Newlands ES, Stevens MF, Wedge SR, Wheelhouse RT, Brock C. Temozolomide: a review of its discovery, chemical properties, pre-clinical development and clinical trials. Cancer treatment reviews. 1997 Jan;23(1):35-61. PubMed PMID: 9189180.

6. Stupp R, Gander M, Leyvraz S, Newlands E. Current and future developments in the use of temozolomide for the treatment of brain tumours. The Lancet Oncology. 2001 Sep;2(9):552-60. PubMed PMID: 11905710.

7. Ohka F, Natsume A, Wakabayashi T. Current trends in targeted therapies for glioblastoma multiforme. Neurology research international. 2012;2012:878425. PubMed PMID: 22530127. Pubmed Central PMCID: 3317017.

8. Lamszus K, Kunkel P, Westphal M. Invasion as limitation to anti-angiogenic glioma therapy. Acta neurochirurgica Supplement. 2003;88:169-77. PubMed PMID: 14531575.

9. Corsten MF, Shah K. Therapeutic stem-cells for cancer treatment: hopes and hurdles in tactical warfare. The Lancet Oncology. 2008 Apr;9(4):376-84. PubMed PMID: 18374291.

10. Pereboeva L, Komarova S, Mikheeva G, Krasnykh V, Curiel DT. Approaches to utilize mesenchymal progenitor cells as cellular vehicles. Stem cells. 2003;21(4):389-404. PubMed PMID: 12832693.

11. Colter DC, Class R, DiGirolamo CM, Prockop DJ. Rapid expansion of recycling stem cells in cultures of plastic-adherent cells from human bone marrow. Proceedings of the National Academy of Sciences of the United States of America. 2000 Mar 28;97(7):3213-8. PubMed PMID: 10725391. Pubmed Central PMCID: 16218.

12. Sekiya I, Larson BL, Smith JR, Pochampally R, Cui JG, Prockop DJ. Expansion of human adult stem cells from bone marrow stroma: conditions that maximize the yields of early progenitors and evaluate their quality. Stem cells. 2002;20(6):530-41. PubMed PMID: 12456961.

13. Fouillard L, Chapel A, Bories D, Bouchet S, Costa JM, Rouard H, et al. Infusion of allogeneic-related HLA mismatched mesenchymal stem cells for the treatment of incomplete engraftment following autologous haematopoietic stem cell transplantation. Leukemia. 2007 Mar;21(3):568-70. PubMed PMID: 17252011.

14. Marmont AM, Gualandi F, Piaggio G, Podesta M, Teresa van Lint M, Bacigalupo A, et al. Allogeneic bone marrow transplantation (BMT) for refractory Behcet's disease with severe CNS involvement. Bone marrow transplantation. 2006 Jun;37(11):1061-3. PubMed PMID: 16633360.

15. Le Blanc K, Ringden O. Immunobiology of human mesenchymal stem cells and future use in hematopoietic stem cell transplantation. Biology of blood and marrow transplantation : journal of the American Society for Blood and Marrow Transplantation. 2005 May;11(5):321-34. PubMed PMID: 15846285.

16. Ripa RS, Haack-Sorensen M, Wang Y, Jorgensen E, Mortensen S, Bindslev L, et al. Bone marrow derived mesenchymal cell mobilization by granulocyte-colony stimulating factor after acute myocardial infarction: results from the Stem Cells in Myocardial Infarction (STEMMI) trial. Circulation. 2007 Sep 11;116(11 Suppl):I24-30. PubMed PMID: 17846310.

17. Chen SL, Fang WW, Ye F, Liu YH, Qian J, Shan SJ, et al. Effect on left ventricular function of intracoronary transplantation of autologous bone marrow mesenchymal stem cell in patients with acute myocardial infarction. The American journal of cardiology. 2004 Jul 1;94(1):92-5. PubMed PMID: 15219514.

18. Park JS, Chang DY, Kim JH, Jung JH, Park J, Kim SH, et al. Retrovirus-mediated transduction of a cytosine deaminase gene preserves the stemness of mesenchymal stem cells. Experimental & molecular medicine. 2013;45:e10. PubMed PMID: 23429359. Pubmed Central PMCID: 3584665.

19. Koppula PR, Chelluri LK, Polisetti N, Vemuganti GK. Histocompatibility testing of cultivated human bone marrow stromal cells - a promising step towards pre-clinical screening for allogeneic stem cell therapy. Cellular immunology. 2009;259(1):61-5. PubMed PMID: 19577229.

20. Studeny M, Marini FC, Champlin RE, Zompetta C, Fidler IJ, Andreeff M. Bone marrow-derived mesenchymal stem cells as vehicles for interferon-beta delivery into tumors. Cancer research. 2002 Jul 1;62(13):3603-8. PubMed PMID: 12097260.

21. Gao H, Priebe W, Glod J, Banerjee D. Activation of signal transducers and activators of transcription 3 and focal adhesion kinase by stromal cell-derived factor 1 is required for migration of human mesenchymal stem cells in response to tumor cell-conditioned medium. Stem cells. 2009 Apr;27(4):857-65. PubMed PMID: 19350687.

22. Ponte AL, Marais E, Gallay N, Langonne A, Delorme B, Herault O, et al. The in vitro migration capacity of human bone marrow mesenchymal stem cells: comparison of chemokine and growth factor chemotactic activities. Stem cells. 2007 Jul;25(7):1737-45. PubMed PMID: 17395768.

23. Aboody KS, Najbauer J, Metz MZ, D'Apuzzo M, Gutova M, Annala AJ, et al. Neural stem cell-mediated enzyme/prodrug therapy for glioma: preclinical studies. Science translational medicine. 2013 May 8;5(184):184ra59. PubMed PMID: 23658244. Pubmed Central PMCID: 3864887.

24. Mesnil M, Yamasaki H. Bystander effect in herpes simplex virus-thymidine kinase/ganciclovir cancer gene therapy: role of gap-junctional intercellular communication. Cancer research. 2000 Aug 1;60(15):3989-99. PubMed PMID: 10945596.

25. Gambhir SS, Barrio JR, Phelps ME, Iyer M, Namavari M, Satyamurthy N, et al. Imaging adenoviral-directed reporter gene expression in living animals with positron emission tomography. Proceedings of the National Academy of Sciences of the United States of America. 1999 Mar 2;96(5):2333-8. PubMed PMID: 10051642. Pubmed Central PMCID: 26784.

26. Kim SM, Woo JS, Jeong CH, Ryu CH, Lim JY, Jeun SS. Effective combination therapy for malignant glioma with TRAIL-secreting mesenchymal stem cells and lipoxygenase inhibitor MK886. Cancer research. 2012 Sep 15;72(18):4807-17. PubMed PMID: 22962275.

27. Sasportas LS, Kasmieh R, Wakimoto H, Hingtgen S, van de Water JA, Mohapatra G, et al. Assessment of therapeutic efficacy and fate of engineered human mesenchymal stem cells for cancer therapy. Proceedings of the National Academy of Sciences of the United States

of America. 2009 Mar 24;106(12):4822-7. PubMed PMID: 19264968. Pubmed Central PMCID: 2660771.

28. Xing L, Sun X, Deng X, Kotedia K, Zanzonico PB, Ackerstaff E, et al. A triple suicide gene strategy that improves therapeutic effects and incorporates multimodality molecular imaging for monitoring gene functions. Cancer gene therapy. 2013 Jun;20(6):358-65. PubMed PMID: 23722591. Pubmed Central PMCID: 3696018.

29. Longley DB, Harkin DP, Johnston PG. 5-fluorouracil: mechanisms of action and clinical strategies. Nature reviews Cancer. 2003 May;3(5):330-8. PubMed PMID: 12724731.

30. Trinh QT, Austin EA, Murray DM, Knick VC, Huber BE. Enzyme/prodrug gene therapy: comparison of cytosine deaminase/5-fluorocytosine versus thymidine kinase/ganciclovir enzyme/prodrug systems in a human colorectal carcinoma cell line. Cancer research. 1995 Nov 1;55(21):4808-12. PubMed PMID: 7585511.

31. Ramnaraine M, Pan W, Goblirsch M, Lynch C, Lewis V, Orchard P, et al. Direct and bystander killing of sarcomas by novel cytosine deaminase fusion gene. Cancer research. 2003 Oct 15;63(20):6847-54. PubMed PMID: 14583482.

32. Parekkadan B, Milwid JM. Mesenchymal stem cells as therapeutics. Annual review of biomedical engineering. 2010 Aug 15;12:87-117. PubMed PMID: 20415588. Pubmed Central PMCID: 3759519.

33. Aboody KS, Brown A, Rainov NG, Bower KA, Liu S, Yang W, et al. Neural stem cells display extensive tropism for pathology in adult brain: evidence from intracranial gliomas. Proceedings of the National Academy of Sciences of the United States of America. 2000 Nov 7;97(23):12846-51. PubMed PMID: 11070094. Pubmed Central PMCID: 18852.

34. Kang JH, Chung JK. Molecular-genetic imaging based on reporter gene expression. Journal of nuclear medicine : official publication, Society of Nuclear Medicine. 2008 Jun;49 Suppl 2:164S-79S. PubMed PMID: 18523072.

35. Alieva M, Bago JR, Aguilar E, Soler-Botija C, Vila OF, Molet J, et al. Glioblastoma therapy with cytotoxic mesenchymal stromal cells optimized by bioluminescence imaging of tumor and therapeutic cell response. PloS one. 2012;7(4):e35148. PubMed PMID: 22529983. Pubmed Central PMCID: 3328467.

36. Zhu Q, Tannenbaum S, Hegde P, Kane M, Xu C, Kurtzman SH. Noninvasive monitoring of breast cancer during neoadjuvant chemotherapy using optical tomography with ultrasound

localization. Neoplasia. 2008 Oct;10(10):1028-40. PubMed PMID: 18813360. Pubmed Central PMCID: 2546597.

37. Ginsberg LE, Fuller GN, Hashmi M, Leeds NE, Schomer DF. The significance of lack of MR contrast enhancement of supratentorial brain tumors in adults: histopathological evaluation of a series. Surgical neurology. 1998 Apr;49(4):436-40. PubMed PMID: 9537664.

38. Schlemmer HP, Pichler BJ, Schmand M, Burbar Z, Michel C, Ladebeck R, et al. Simultaneous MR/PET imaging of the human brain: feasibility study. Radiology. 2008 Sep;248(3):1028-35. PubMed PMID: 18710991.

39. Lunsford LD, Martinez AJ, Latchaw RE. Magnetic resonance imaging does not define tumor boundaries. Acta radiologica Supplementum. 1986;369:154-6. PubMed PMID: 2980437.

40. Kumar AJ, Leeds NE, Fuller GN, Van Tassel P, Maor MH, Sawaya RE, et al. Malignant gliomas: MR imaging spectrum of radiation therapy- and chemotherapy-induced necrosis of the brain after treatment. Radiology. 2000 Nov;217(2):377-84. PubMed PMID: 11058631.

41. Ulmer S, Braga TA, Barker FG, 2nd, Lev MH, Gonzalez RG, Henson JW. Clinical and radiographic features of peritumoral infarction following resection of glioblastoma. Neurology. 2006 Nov 14;67(9):1668-70. PubMed PMID: 17101902.

42. Alavi JB, Alavi A, Chawluk J, Kushner M, Powe J, Hickey W, et al. Positron emission tomography in patients with glioma. A predictor of prognosis. Cancer. 1988 Sep 15;62(6):1074-8. PubMed PMID: 3261622.

43. Wong TZ, van der Westhuizen GJ, Coleman RE. Positron emission tomography imaging of brain tumors. Neuroimaging clinics of North America. 2002 Nov;12(4):615-26. PubMed PMID: 12687915.

44. Ricci PE, Karis JP, Heiserman JE, Fram EK, Bice AN, Drayer BP. Differentiating recurrent tumor from radiation necrosis: time for re-evaluation of positron emission tomography? AJNR American journal of neuroradiology. 1998 Mar;19(3):407-13. PubMed PMID: 9541290.

45. Zhao S, Kuge Y, Yi M, Zhao Y, Hatano T, Magota K, et al. Dynamic 11C-methionine PET analysis has an additional value for differentiating malignant tumors from granulomas: an experimental study using small animal PET. European journal of nuclear medicine and molecular imaging. 2011 Oct;38(10):1876-86. PubMed PMID: 21732106.

46. Jacobs AH, Thomas A, Kracht LW, Li H, Dittmar C, Garlip G, et al. 18F-fluoro-L-thymidine and 11C-methylmethionine as markers of increased transport and proliferation in brain tumors. Journal of nuclear medicine : official publication, Society of Nuclear Medicine. 2005 Dec;46(12):1948-58. PubMed PMID: 16330557.

47. Chung JK, Kim YK, Kim SK, Lee YJ, Paek S, Yeo JS, et al. Usefulness of 11C-methionine PET in the evaluation of brain lesions that are hypo- or isometabolic on 18F-FDG PET. European journal of nuclear medicine and molecular imaging. 2002 Feb;29(2):176-82. PubMed PMID: 11926379.

48. Goldman S, Levivier M, Pirotte B, Brucher JM, Wikler D, Damhaut P, et al. Regional methionine and glucose uptake in high-grade gliomas: a comparative study on PET-guided stereotactic biopsy. Journal of nuclear medicine : official publication, Society of Nuclear Medicine. 1997 Sep;38(9):1459-62. PubMed PMID: 9293808.

49. Pirotte B, Goldman S, David P, Wikler D, Damhaut P, Vandesteene A, et al. Stereotactic brain biopsy guided by positron emission tomography (PET) with [F-18]fluorodeoxyglucose and [C-11]methionine. Acta neurochirurgica Supplement. 1997;68:133-8. PubMed PMID: 9233429.

50. Chang DY, Yoo SW, Hong Y, Kim S, Kim SJ, Yoon SH, et al. The growth of brain tumors can be suppressed by multiple transplantation of mesenchymal stem cells expressing cytosine deaminase. International journal of cancer Journal international du cancer. 2010 Oct 15;127(8):1975-83. PubMed PMID: 20473873.

51. Ji JF, He BP, Dheen ST, Tay SS. Interactions of chemokines and chemokine receptors mediate the migration of mesenchymal stem cells to the impaired site in the brain after hypoglossal nerve injury. Stem cells. 2004;22(3):415-27. PubMed PMID: 15153618.

52. Klopp AH, Spaeth EL, Dembinski JL, Woodward WA, Munshi A, Meyn RE, et al. Tumor irradiation increases the recruitment of circulating mesenchymal stem cells into the tumor microenvironment. Cancer research. 2007 Dec 15;67(24):11687-95. PubMed PMID: 18089798. Pubmed Central PMCID: 4329784.

53. Satake K, Lou J, Lenke LG. Migration of mesenchymal stem cells through cerebrospinal fluid into injured spinal cord tissue. Spine. 2004 Sep 15;29(18):1971-9. PubMed PMID: 15371697.

54. Peters GJ, Backus HH, Freemantle S, van Triest B, Codacci-Pisanelli G, van der Wilt CL, et al. Induction of thymidylate synthase as a 5-fluorouracil resistance mechanism. Biochimica et biophysica acta. 2002 Jul 18;1587(2-3):194-205. PubMed PMID: 12084461.

55. Urick ME, Chung EJ, Shield WP, 3rd, Gerber N, White A, Sowers A, et al. Enhancement of 5-fluorouracil-induced in vitro and in vivo radiosensitization with MEK inhibition. Clinical cancer research : an official journal of the American Association for Cancer Research. 2011 Aug 1;17(15):5038-47. PubMed PMID: 21690569. Pubmed Central PMCID: 3149743.

56. Preul MC, Caramanos Z, Collins DL, Villemure JG, Leblanc R, Olivier A, et al. Accurate, noninvasive diagnosis of human brain tumors by using proton magnetic resonance spectroscopy. Nature medicine. 1996 Mar;2(3):323-5. PubMed PMID: 8612232.

57. Wolf W, Presant CA, Waluch V. 19F-MRS studies of fluorinated drugs in humans. Advanced drug delivery reviews. 2000 Mar 15;41(1):55-74. PubMed PMID: 10699305.

58. Brandsma D, van den Bent MJ. Pseudoprogression and pseudoresponse in the treatment of gliomas. Current opinion in neurology. 2009 Dec;22(6):633-8. PubMed PMID: 19770760.

59. Hygino da Cruz LC, Jr., Rodriguez I, Domingues RC, Gasparetto EL, Sorensen AG. Pseudoprogression and pseudoresponse: imaging challenges in the assessment of posttreatment glioma. AJNR American journal of neuroradiology. 2011 Dec;32(11):1978-85. PubMed PMID: 21393407.

60. Zhou J, Tryggestad E, Wen Z, Lal B, Zhou T, Grossman R, et al. Differentiation between glioma and radiation necrosis using molecular magnetic resonance imaging of endogenous proteins and peptides. Nature medicine. 2011 Jan;17(1):130-4. PubMed PMID: 21170048. Pubmed Central PMCID: 3058561.

61. Heiss WD, Raab P, Lanfermann H. Multimodality assessment of brain tumors and tumor recurrence. Journal of nuclear medicine : official publication, Society of Nuclear Medicine. 2011 Oct;52(10):1585-600. PubMed PMID: 21840931.

62. Weber DC, Zilli T, Buchegger F, Casanova N, Haller G, Rouzaud M, et al. [(18)F]Fluoroethyltyrosine- positron emission tomography-guided radiotherapy for high-grade glioma. Radiation oncology. 2008;3:44. PubMed PMID: 19108742. Pubmed Central PMCID: 2628662.

63. Nariai T, Tanaka Y, Wakimoto H, Aoyagi M, Tamaki M, Ishiwata K, et al. Usefulness of L-[methyl-11C] methionine-positron emission tomography as a biological monitoring tool in the treatment of glioma. Journal of neurosurgery. 2005 Sep;103(3):498-507. PubMed PMID: 16235683.

64. Grosu AL, Weber WA, Riedel E, Jeremic B, Nieder C, Franz M, et al. L-(methyl-11C) methionine positron emission tomography for target delineation in resected high-grade

gliomas before radiotherapy. International journal of radiation oncology, biology, physics. 2005 Sep 1;63(1):64-74. PubMed PMID: 16111573.

65. Lucignani G. SUV and segmentation: pressing challenges in tumour assessment and treatment. European journal of nuclear medicine and molecular imaging. 2009 Apr;36(4):715-20. PubMed PMID: 19205697.

66. Espinosa E, Zamora P, Feliu J, Gonzalez Baron M. Classification of anticancer drugs--a new system based on therapeutic targets. Cancer treatment reviews. 2003 Dec;29(6):515-23. PubMed PMID: 14585261.

67. Longley DB, Johnston PG. Molecular mechanisms of drug resistance. The Journal of pathology. 2005 Jan;205(2):275-92. PubMed PMID: 15641020.

68. Zhou BB, Bartek J. Targeting the checkpoint kinases: chemosensitization versus chemoprotection. Nature reviews Cancer. 2004 Mar;4(3):216-25. PubMed PMID: 14993903.

69. Ando T, Ishiguro H, Kuwabara Y, Kimura M, Mitsui A, Sugito N, et al. Relationship between expression of 5-fluorouracil metabolic enzymes and 5-fluorouracil sensitivity in esophageal carcinoma cell lines. Diseases of the esophagus : official journal of the International Society for Diseases of the Esophagus / ISDE. 2008;21(1):15-20. PubMed PMID: 18197934.

70. Ide H, Kikuchi E, Hasegawa M, Kozakai N, Kosaka T, Miyajima A, et al. Prognostic significance of 5-fluorouracil metabolism-relating enzymes and enhanced chemosensitivity to 5-fluorouracil by 5-chloro 2,4-dihydroxy-pyridine in urothelial carcinoma. BMC cancer. 2012;12:420. PubMed PMID: 22998564. Pubmed Central PMCID: 3522564.

71. Tyner JW. Functional genomics for personalized cancer therapy. Science translational medicine. 2014 Jul 2;6(243):243fs26. PubMed PMID: 24990879.

국문 초록

서론: 악성 뇌교종은 기존의 항암치료에도 불구하고 광범위한 암 침윤 때문에 완치가 드물고 환자의 생존율이 매우 낮다. 중간엽 줄기세포는 암세포를 표적 치료할 수 있기 때문에 줄기세포를 이용한 항암 연구가 전 세계적으로 진행 중이다. 이 연구에서는 비활성 약제 5-플루오로시토신과 함께 시토신 디아미나아제를 발현하는 중간엽 줄기세포를 이용하여 뇌종양 세포에 대한 치료효과를 분자 영상 실험을 이용하여 확인하였다.

방법: 사람 신경교종 세포 주 (U87MG, U373)와 신경교종 환자의 조직으로부터 동정한 신경교종세포 (GBM28)를 영상화 하기 위해서 형광 유전자와 생체발광 유전자를 신경교종 세포에 이입하였다. 표준 신경교종 치료방법인 비전리 방사선 또는 테모졸로마이드를 신경교종 세포에 처리한 후 세포독성을 생체발광 영상을 통하여 관찰 및 정량화 하였다. 각 신경교종 세포의 세포독성 차이의 원인을 찾기 위해 방사선 치료에 저항성을 갖도록 하는 DNA 회복 경로 연관 유전자의 발현을 마이크로어레이 유전자 분석을 통하여 비교 확인하였다. 또한 5-플루오로시토신의 활성 약제인 5-플루오로우라실에 의한 신경교종 세포의 세포독성을 확인 한 후 유전자 분석을 통하여 5-플루오로우라실 대사관련 유전자의 발현을 비교 확인하였다. 인간 골수 유래 중간엽 줄기세포에 시토신 디아미나아제 유전자를 이입하여 시토신 디아미나아제를 발현하는 치료용 줄기세포를 제작하고 형광 유전자와 생체발광 유전자를 이입하여 영상화 하였다. 시토신 디아미나제 발현 줄기세포에 의한 5-플루오로시토신의 5-플루오로우라실 전환을 핵자기 공명 실험을 이용하여 확인하였고 치료용 줄기세포의 항암효과를 세포와 마우스 생체 내에서 확인하였다.

결과: 비전리 방사선(3 Gy)에 의해서 U87MG 의 경우 82.8% ± 9.59% 의 생존율을 보였고 U373 과 GBM28 의 경우 57.9% ± 6.88%, 48.0 ± 6.0%의 세포 생존율을 생체발광 영상을 통하여 확인하였다. 방사선 저항성에 영향을 주는 DNA

회복 경로와 관련된 유전자들이 U373, GBM28 세포에 비하여 U87MG 세포가 강하게 발현되는 것을 확인하였다. 4 uM 의 5-플루오로우라실 처리 시, U87MG 신경교종 세포는 36.3% ± 8.9%의 생존율을 보이는 반면 U373 은 68.6% ± 15% 의 생존율을 보였다. 유전자 분석을 통하여 U87MG 세포가 5-플루오로우라실 활성에 영향을 주는 디하이드로피리미딘 탈수소 효소의 발현이 U373 세포 보다 적은 것을 알 수 있었다. 핵자기 공명 실험을 이용하여 시토신 디아미나제 발현 줄기세포에 의한 5-플루오로시토신의 5-플루오로우라실 전환을 확인하였고 시토신 디아미나제 발현 줄기세포와 신경교종 세포를 함께 배양하였을 때, 5-FC 의 농도에 따라서 신경교종 세포에 대한 세포독성 효과를 확인할 수 있었다. 50 uM 의 5-플루오로시토신 처리 시, U87MG 세포는 82.5% ± 0.69%, U373 의 경우 65.1% ± 7.55% 의 세포독성 효과를 관찰하였다. 뇌종양 마우스 모델에서 생체발광영상, 자기공명영상, 핵의학 영상을 통하여 신경교종세포의 성장이 시토신 디아미나제 발현 줄기세포와 5-플루오로시토신에 의하여 70%가 감소하는 것을 확인할 수 있었다.

결론: 시토신 디아미나제 발현 줄기세포와 5-플루오로시토신에 의한 악성 뇌교종 세포의 치료효과를 분자 영상을 이용하여 확인하였다. 생체 발광 영상 이용 시, 세포 실험과 원발성 뇌종양 마우스 모델 모두에서 줄기세포에 의한 치료효과를 정확하게 확인 할 수 있었으며 악성 뇌교종 세포가 발현하는 유전자 차이에 의해서 치료법에 따른 민감성이 다르게 나타나는 것을 알 수 있었다. 그러므로 이 연구에서 사용한 시토신 디아미나제 발현 줄기세포와 5-플루오로시토신 치료제는 방사선에 저항성이 있으며 5-플루오로우라실에 민감한 악성 뇌교종 세포 치료제 개발에 크게 기여할 수 있을 것으로 사료된다.

주요어 : 신경교종세포, 중간엽 줄기세포, 5-fluorouracil, 5-Fluorocytosine, Cytosine deaminase

학 번 : 2011-30634